Generation of Macromolecule-Templated Gold Nanoparticles

by Ionizing Radiation

by

Candace Walker

A Thesis Presented in Partial Fulfillment
of the Requirements for the Degree
Master of Science

Approved November 2012 by the
Graduate Supervisory Committee:

Kaushal Rege, Chair
John Chang
Potta Thrimoorthy
Vikram Kodibagkar

ARIZONA STATE UNIVERSITY

December 2012

ABSTRACT

Ionizing radiation, such as gamma rays and X-rays, are becoming more widely used. These high-energy forms of electromagnetic radiation are present in nuclear energy, astrophysics, and the medical field. As more and more people have the opportunity to be exposed to ionizing radiation, the necessity for coming up with simple and quick methods of radiation detection is increasing. In this work, two systems were explored for their ability to simply detect ionizing radiation. Gold nanoparticles were formed via radiolysis of water in the presence of Elastin-like polypeptides (ELPs) and also in the presence of cationic polymers. Gold nanoparticle formation is an indicator of the presence of radiation. The system with ELP was split into two subsystems: those samples including isopropyl alcohol (IPA) and acetone, and those without IPA and acetone. The samples were exposed to certain radiation doses and gold nanoparticles were formed. Gold nanoparticle formation was deemed to have occurred when the sample changed color from light yellow to a red or purple color. Nanoparticle formation was also checked by absorbance measurements. In the cationic polymer system, gold nanoparticles were also formed after exposing the experimental system to certain radiation doses. Unique to the polymer system was the ability of some of the cationic polymers to form gold nanoparticles without the samples being irradiated. Future work to be done on this project is further characterization of the gold nanoparticles formed by both systems.

ACKNOWLEDGMENTS

I would like to thank a few people who helped me complete this work. First, Dr. Kaushal Rege, my PI and academic advisor, thank you for allowing me to join the laboratory and for the support and advice given through the last year. I would like to thank my past and current laboratory group members for all of their assistance and help with various tasks and projects and for also making me feel welcome in the group. Thank you, Dr. Thrimoorthy Potta, for your assistance with polymer chemistry and also for agreeing to be on my thesis committee.

Next, I would like to thank Dr. John Chang, Dr. Steve Sapareto, Dr. Tomasz Bista, and Thaddeus Sokolowski at the Banner MD Anderson Cancer Center for all of their help running the radiation experiments. A special thanks goes to Dr. Chang for setting up the collaboration and for agreeing to be a member of my thesis committee. Also, thank you to Dr. Vikram Kodibagkar for lending me valuable reference material and for agreeing to be a member on my thesis committee.

Finally, I would like to thank my families, here in the Phoenix area and back home in New Mexico, for all of their love, prayers, and support through the past several months. I could not have gotten through the last couple of months without you.

TABLE OF CONTENTS

Page

CHAPTER Page

CHAPTER Page

LIST OF FIGURES

Chapter 1

INTRODUCTION

1.1 Background

Ionizing radiation, like X-rays and gamma rays, exist in many areas, including nuclear power, astrophysics, and the medical industries. X-rays and gamma rays are both forms of electromagnetic radiation, meaning they consist of photons. They both exhibit high energy and have wavelengths in the same range. The difference between them is that gamma rays originate from within the nucleus of an atom and X-rays originate from outside the nucleus (electrons) of an atom (Washington & Leaver, 2010). X-rays and gamma rays are indistinguishable from one another unless the source of the radiation is known. Ionizing radiation poses a threat to human health. Radicals formed due to radiolysis of water can damage DNA via single or double strand breaks. If the strand breaks are improperly repaired, alterations to chromosomes may happen, leading to mutations (Lahtz et. al, 2012). It is, therefore, very important to develop methods to detect these ionizing radiations.

There are several methods reported for detecting gamma radiation. These include superheated droplets, nanophosphors, CdTe, CdZnTe, graphenes, inorganic-organic structures, and flouresence-detection methods (Liu et. al, 2011). There are, however, drawbacks associated with each of these methods. It is, therefore, necessary to come up with a detection method that is simple and convenient to use, without the necessity of special equipment to determine

if radiation is present in a given situation. Presented is a visual based detection method of gamma radiation or X-rays based on the formation of gold nanoparticles Templated with ELPs or cationic polymers.

1.2 Elastin-like Polypeptides

Elaslin-like polypeptides (ELPs) are recombinant peptides that mimic mammalian elastin. ELPs have the repetitive amino acid sequence $(VPGXG)_n$, where X is any amino acid except proline (Urry, 1997). ELPs are soluble in aqueous media below the transition temperature because they are hydrated fully. ELPs have been demonstrated to interact with metallic gold for applications such as sensing (Huang et. al, 2008, Huang et. al, 2011, Nath et. al, 2011). ELPs with two cysteines in the amino acid repeat sequence have been interfaced with gold nanorods due to the gold-thiol bonds (Huang et. al, 2008). Raising the solution temperature to that above the transition temperature of the ELP, results in the formation of ELP-gold nanorod nanoassemblies (Huang et. al, 2008). The known interactive properties of ELPs with gold therefore made ELPs an interesting candidate for use with radiation detection.

1.3 Conclusion

The ever-growing use of radiation in society means that detection methods need to become simple enough for anyone to use them. The methods presented here fulfill this necessity to come up with simple methods to detect gamma radiation and X-rays as the detection mechanism is via a color change.

Chapter 2

CNELP SYNTHESIS AND GENERATION OF CNELP-TEMPLATED GOLD NANOPARTICLES BY IONIZING RADIATION

2.1 Introduction

Elastin-like polypeptides (ELPs) readily interact with metallic gold due to gold-thiol interactions (Huang et. al, 2008). When water is exposed to an ionizing radiation, such as gamma rays or X-rays, it is split into reactive species H·, ·OH, and e_{aq}- (Misra et. al, 2012). These reactive species are able to reduce metallic gold to a zero valence state, resulting in gold nanoparticles. If ELP is present in the system, it will bind to the surface of the gold nanoparticle due to gold-thiol bonds. The ELP can act as a capping agent which adds stability to the gold nanoparticles formed after irradiation.

In this work, four experimental systems were set up. Two different ELPs, C_2ELP and C_{12}ELP, were mixed with metallic gold and nanopure water. These ELPs were also mixed with isopropyl alcohol and acetone, along with the metallic gold and nanopure water. The four systems were then irradiated using a linear accelerator to different radiation doses and evaluated for forming gold nanoparticles.

2.2 Materials and Methods

2.2.1 Materials. Gold(III) chloride trihydrate ($HAuCl_4 \cdot 3H_2O$) was purchased from Sigma-Aldrich. Isopropyl alcohol (IPA) (99.5%) was purchased from BDH. Acetone was purchased from Lab Safety Supply Inc and Reductacryl

resin was purchased from EMD. All chemicals were used as received from the manufacturer without any additional purification.

2.2.2 Synthesis, Expression, and Purification of Elastin-like Polypeptides (ELPs). An Elastin-like polypeptide, containing two or twelve cysteine residues (C_2ELP orC_{12}ELP) in the repetitive sequence, MVSACRGPG-(VG VPGVGVPGVGVPGVGVPGVGVPG)$_8$-(VGVPGVG VPGVG VPGCG VPGVG VPG)$_n$-WP, where n is equal to two or twelve, was generated via recursive directional ligation (Meyer et. al, 2002); the C_2 or C_{12} in the C_2ELP or C_{12}ELP name indicates the presence of two or twelve cysteines in the ELP repeat sequence. Oligonucleotides encoding the ELPs were first cloned into pUC19, followed by cloning into a modified version of the pET25b+expression vector at the sfiI site. *Escherichia coli* BLR(DE3) (Novagen)was used as a bacterial host for polypeptide expression, followed by purification and lyophilization, and stored at 4 °C as described previously (Huang et. al, 2008).

2.2.3 Preparation of C_nELP Samples. C_nELP bulk samples were prepared by dissolving the ELP in nanopure water (18.2 MΩ-cm, resistivity) to a concentration of 1mg/mL. Reductacryl resin was added to the ELP in amounts of 1 mg/mL. Reductacryl was added in order to reduce the cysteines in the polypeptide chain. The samples mixed for at least 30 minutes under constant rotation at 4°C. After 30 minutes, the Reductacryl resin was removed from the dissolved ELP via centrifugation at 6000 rcf for 10 minutes. Reduced ELP bulk samples were stored at 4°C until used.

2.2.4 Preparation of Samples for Irradiation. Two sets of samples were prepared. The first sample set comprised of $HAuCl_4$ ($1x10^{-3}$M), C_nELP, where n=2 or n=12, (0.1% w/v), isopropyl alcohol (IPA) (0.2M), acetone (0.058M), and the balance nanopure water (18.2 MΩ-cm, resistivity). The second sample set comprised of the same components as the first, minus the isopropyl alcohol and the acetone. Samples were mixed immediately prior to irradiation.

2.2.5 Sample Irradiation. Samples were transported to the Banner MD Anderson Cancer Center for irradiation tests. A Truebeam linear accelerator irradiated the samples to different doses, at a dose rate of ~15Gy/minute. The doses were 0.5Gy, 2Gy, 5Gy, 10Gy, 25Gy, 50Gy, 100Gy, 175Gy, 200Gy, 268Gy, 536Gy, 804Gy, and 1072Gy. After irradiation, samples were transported back to the lab for characterization.

2.2.6 Absorbance Spectroscopy. After irradiation, the absorbance spectra of the samples were measured. The absorbance was measured using a BioTek plate reader and Gen5 software. Absorbance measurements were read from 300nm to 995nm, with a step size of 5nm in a 96 well plate, with 150uL of sample in each well. The absorbance was measured at ~1 hour post irradiation and ~18 hours post irradiation.

2.2.7 Particle Size Determination. Particle size was determined using dynamic light scattering (DLS). DLS was performed on a Dynamic Light Scattering Particle Sizer (Corrvus Advanced Optical Instruments) using Corcle software. The analyzed sample was placed in a square 1mL cuvette and placed into the instrument. The software was set up to do sample measurements with

auto-correlation. The data was collected for 1 minute per sample and hydrodynamic diameter was determined.

2.2.8 Particle Surface Charge Determination. The surface charge of the nanoparticles was determined via zeta potential measurements. The zeta potential measurements were conducted on a Beckman Coulter Delsa^{TM} Nano C Particle Analyzer. The instrument was turned on and left to warm up for five minutes. The software "Delsa Nano 3.73" and standard SOP 'Zeta1' were used for all zeta potential measurements. 400-500µL of solution was pipetted into a 3mL syringe and flown into the flow cell chamber. After placing the chamber inside the instrument, time was given for the intensity bar to turn blue, indicating optimal conditions. In some cases when the intensity did not optimize, the pinhole was increased from 50 to 100µm. The measurement was then started and zeta potential value was recorded after each run. The flow cell chamber was then taken out and solution carefully withdrawn. The flow cell was washed through multiple times with nanopure water between each experiment.

2.2.9 Statistical Analysis. All experiments were done in triplicate. Statistical significance was determined with a student's t-test. A p-value of 0.05 or less was determined to be statistically significant.

2.3 Results and Discussion

2.3.1 Control Experiments. In this study, an investigation was done to determine whether or not gold nanoparticles could be synthesized via radiation, and to determine what factors were necessary to facilitate the nanoparticle

formation. Upon irradiation, aqueous solutions experience radiolysis of water in which free radicals (H· and ·OH) and aqueous electrons (e_{aq}-) are formed.

Different control experiments were conducted to determine factors that would be important in the formation of gold nanoparticles. The control experimental chart is shown in **Figure 1**.

	Cn	**Radiation**	**Gold III**	**IPA/acetone**	**NP Formation**
Control 1	-	+	+	-	no
Control 2	-	+	+	+	no
Control 3	+	-	+	-	no
Control 4	+	-	+	+	no
Control 5	+	+	-	-	no
Control 6	+	+	-	+	no

Figure 1: Control experiments were conducted according to the above chart. C_n denotes the C_nELP, with n equal to 2 or 12. The (+) denotes that the particular component was included in the sample and the (-) denotes that the particular component was excluded. NP denotes nanoparticle.

2.3.2 Gold Nanoparticle Formation. The absorbance spectra for the control experiments are included in **Appendix A**. Two systems were determined to facilitate gold nanoparticle formation: C_nELPs in the presence of gold salt, IPA, acetone, and radiation and C_nELPs in the presence of gold salt and radiation. Gold nanoparticle formation was deemed to occur after radiation exposure. Nanoparticle formation was determined with color change and absorbance spectra measurements. If gold nanoparticles formed, the solution turned from a light

yellow color to a purple or red color, as seen in **Figure 2**. The absorbance spectra also confirmed nanoparticle formation if a peak at ~520nm was observed in the measurement.

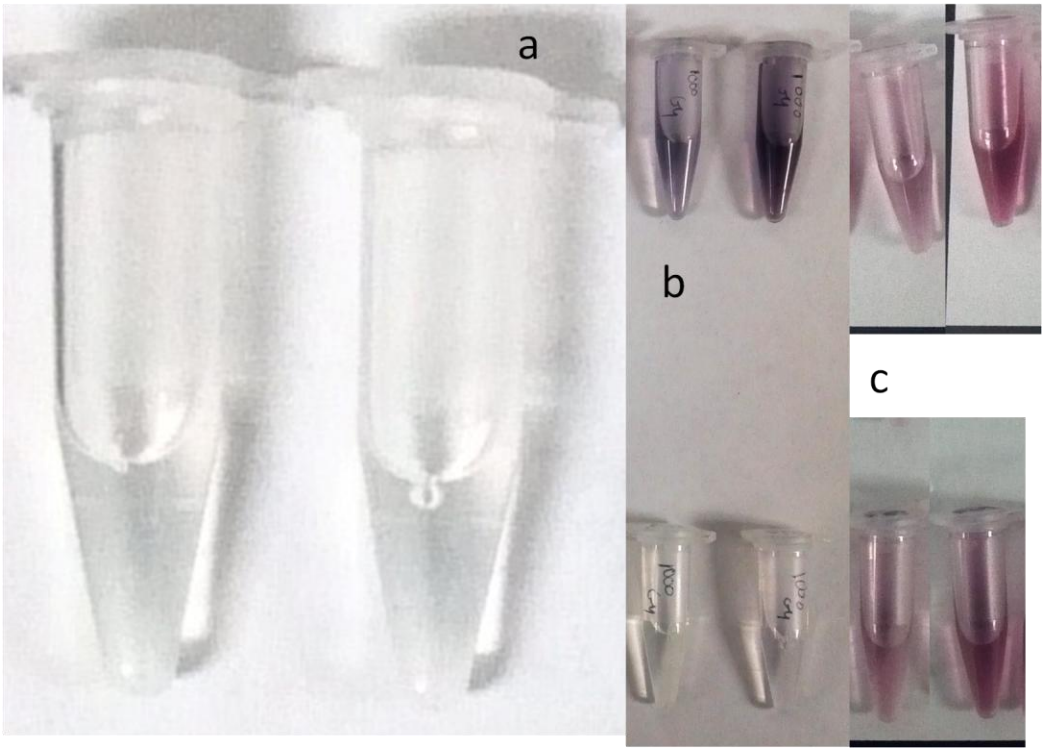

Figure 2: Photographs of CnELPs; a) before exposure to radiation, b) after exposure to 1072Gy of radiation, 1 hour post irradiation, c) after exposure to 1072Gy of radiation, 18 hours post irradiation. The samples in the upper halves of b) and c) correspond to C_2ELP and the lower halves correspond to C_{12}ELP. Going from left to right corresponds to samples without IPA and acetone and samples with IPA and acetone.

2.3.3 Effect of Radiation Dose. The experimental systems were subjected to a variety of radiation doses to determine the minimum dose needed to facilitate gold nanoparticle formation. The doses were 0.5Gy, 2Gy, 5Gy, 10Gy,

25Gy, 50Gy, 100Gy, 175Gy, 200Gy, 268Gy, 536Gy, 804Gy, and 1072Gy. The larger doses have strangely picked doses due to a mistake in calculation, which was not caught until the end of the experiment. The doses were kept consistent throughout the experimental duration, however.

As previously mentioned, gold nanoparticle formation was deemed to have occurred when the solution turned from a light yellow color to a red or purple color. This was confirmed with absorbance spectra measurements. For the lower doses, 0.5Gy to 100Gy, no color change in the sample was noted after irradiation or over the next couple of days. The absorbance spectra measurements confirmed that no gold nanoparticle formation had occurred. A film on the sides of the sample tubes was observed to form, presumably from some surface interactions between the plastic, gold and C_nELPs. Absorbance spectra measurements for the lower-dose experiments are included in **Appendix A**.

The radiation dose was increased to determine the dose in which gold nanoparticle formation would be facilitated. The lowest dose in which gold nanoparticle formation was deemed to have occurred was 175Gy. At this dose, a slight color change was seen 18 hours post irradiation. Particle size determination via dynamic light scattering (DLS) at this dose also confirmed that nanoparticles had formed. The radiation dose was again increased, to200Gy and 268Gy, and multiples thereof. With these higher doses, up to 1072Gy, gold nanoparticle formation was deemed to have occurred due to the color change seen 18 hours post irradiation and was backed up with absorbance spectra measurements and

DLS measurements. The spectra and particle sizes are seen in **Figure 3** and **Figure 4** respectively. Preliminary zeta potential data is in **Appendix A**.

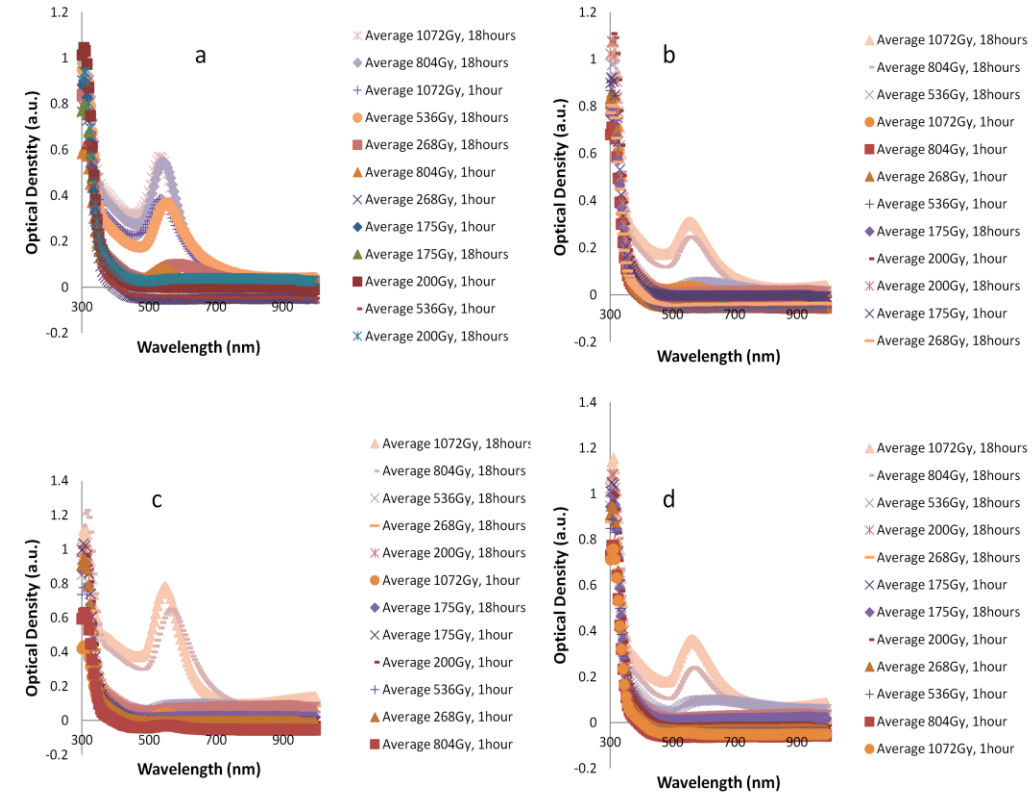

Figure 3: Absorbance spectra measurements for the radiation experiments: a) C_2ELP with Au, IPA, acetone, nanopure water and radiation, b) C_2ELP with Au, nanopure water and radiation, c) C_{12}ELP with Au, IPA, acetone, nanopure water and radiation, d) C_{12}ELP with Au, nanopure water and radiation.

a

none	DLS					
	175Gy	200Gy	268Gy	536Gy	804Gy	1072Gy
	112	112	159	126	49.4	78.8
	141	141	141	126	88.6	88.6
	178		159	112	99.5	88.6
Avg (nm)	143.7	126.5	153.0	121.3	79.2	85.3
Std Dev	33.1	20.5	10.4	8.1	26.3	5.7

b

IPA&ace	DLS					
	175Gy	200Gy	268Gy	536Gy	804Gy	1072Gy
	126	178	159	70.1	34.9	78.8
	159	126	141	112	99.5	49.4
	178		200	88.6	88.6	34.9
Avg (nm)	154.3	152.0	166.7	90.2	74.3	54.4
Std Dev	26.3	36.8	30.2	21.0	34.6	22.4

c

none	DLS					
	175Gy	200Gy	268Gy	536Gy	804Gy	1072Gy
	141	141	126	126	88.6	99.5
	159	178	99.5	112	99.5	88.6
	141	126	159	112	126	88.6
Avg (nm)	147	148.3	128.2	116.7	104.7	92.2
Std Dev	10.4	26.8	29.8	8.1	19.2	6.3

d

IPA&ace	DLS					
	175Gy	200Gy	268Gy	536Gy	804Gy	1072Gy
	178	159	141	126	88.6	99.5
	159	200	178	126	126	88.6
	178	253	141	284	88.6	88.6
Avg (nm)	171.7	204	153.3	178.7	101.1	92.2
Std Dev	11.0	47.1	21.4	91.2	21.6	6.3

Figure 4: Hydrodynamic diameters for gold nanoparticles formed via radiolysis of water for the different experimental systems: a) C_2ELP with Au, IPA, acetone, nanopure water and radiation, b) C_2ELP with Au, nanopure water and radiation, c) $C1_2$ELP with Au, IPA, acetone, nanopure water and radiation, d) C_{12}ELP with Au, nanopure water and radiation. For a) and b), the 200Gy samples have n=2.

An increase in the radiation dose resulted in a deepening of the color observed, so samples that received 1072Gy of radiation would be a darker red or purple color than samples that received 175Gy of radiation. This is presumably due to more 2-propyl radicals present in the system with a higher dose of radiation than the system with lower doses of radiation. More 2-propyl radicals present would be able to reduce more Au^{III} ions, resulting in more gold nanoparticles and thus resulting in a darker color. The effect of radiation dose on gold nanoparticle formation is seen in **Figure 5**.

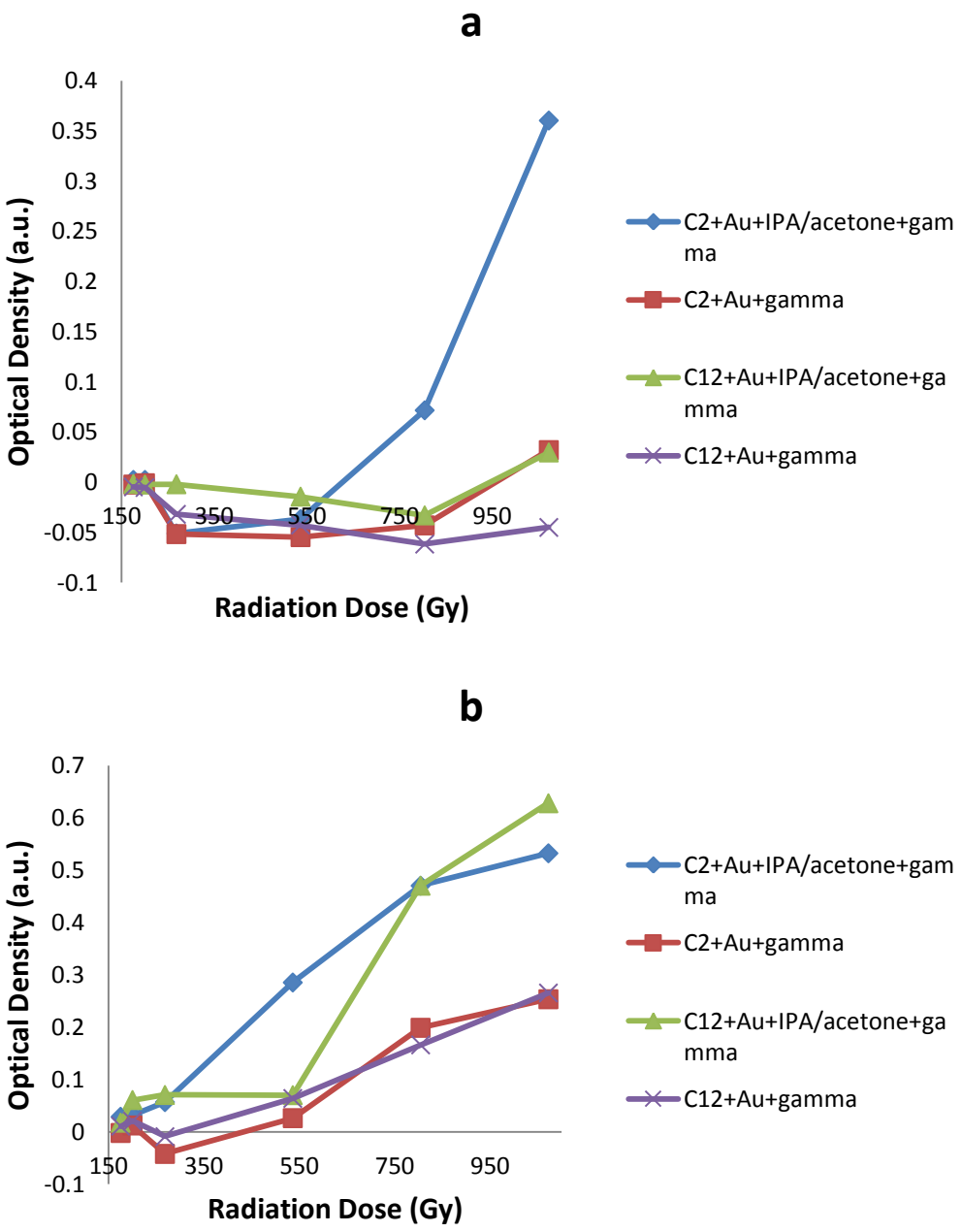

Figure 5: Effect of radiation dose on gold nanoparticle formation. A higher optical density is indicative of more gold nanoparticles formed. All points were taken at 520nm: a) is measured 1 hour after irradiation and b) is measured 18 hours after irradiation. Lines are added for visualization only.

2.3.4 Effect of IPA and Acetone. As mentioned above, H·, ·OH, and e_{aq}- are formed upon radiolysis of water. When IPA and acetone are present in the system, the IPA reacts with the H· and ·OH to give 2-propyl radicals, and the acetone reacts with e_{aq}- to give 2-propyl radicals (Misra et. al, 2012). The 2-propyl radical is able to reduce the Au^{III} ions in the system to their zero valence state, Au^{0}, which leads to formation of gold nanoparticles. The C_nELPs present in the system act as capping agents for the gold nanoparticles. Gold-thiol interactions allow for the attachment of the C_nELPs to the surface of the gold nanoparticles (Huang et. al, 2008).

The two systems which were explored were $HAuCl_4$ in the presence of nanopure water, C_nELP, IPA, and acetone and $HAuCl_4$ in the presence of nanopure water and C_nELP. Each of these systems was subjected to the same doses of radiation. Upon irradiation, it was observed that the systems which included IPA and acetone had darker colors and higher absorbance peaks than systems which did not include IPA and acetone. With these observations, it can be concluded that the 2-propyl radicals present in the systems with IPA and acetone better reduce the Au^{III} ions to the zero valence state than the e_{aq}- present in the systems without IPA and acetone. The e_{aq}- are still able to reduce the Au^{III} ions to the zero valence state to facilitate gold nanoparticle formation, just not as well as the 2-propyl radicals, as seen in **Figure 3**. **Figure 6** shows the difference between the systems with and without IPA and acetone in them.

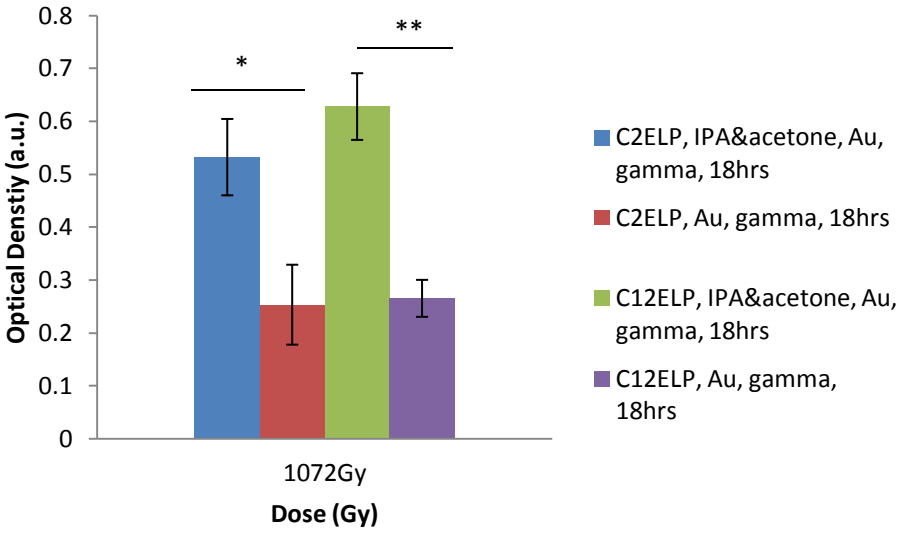

Figure 6: Absorbance spectra values for the different experimental systems at 1072Gy. Statistical significance is determined as follows: *= $p \leq 0.05$, **=$p \leq 0.01$.

2.3.5 Effects of C_2ELP versus C_{12}ELP. The experimental systems also compared two different types of ELPs, C_2ELP and C_{12}ELP. The 2 and 12 in the name denote the number of cysteines present in the ELP chain. As is seen in **Figures 2 and 3**, the system with C_2ELP had a darker color and higher absorbance values than the system with C_{12}ELP, 1 hour after the samples had been irraidiated. This is presumably due to steric hindrance from the number of cysteines present in the ELP sequence.

2.4 Conclusion

In this chapter, gold nanoparticle formation via radiolysis of water was discussed. The gold nanoparticles were Templated with C_nELPs due to gold-thiol interactions. The ELPs helped stabilize the gold nanoparticles upon formation. It was determined that a higher radiation dose, up to 1072Gy, facilitated higher gold nanoparticle formation, as correlated with higher absorbance peaks and darker

solution colors. IPA and acetone also played an important role in gold nanoparticle formation as the systems that included them had higher absorbance peaks and darker color. The number of cysteines present in the amino acid sequence chain also plays a role in gold nanoparticle formation, with fewer cysteines resulting in higher absorbance peaks and darker color. Based on the data here, these C_nELP/gold systems hold promise in detecting high energy radiation like gamma rays and X-rays.

Chapter 3

CATIONIC POLYMER SYNTHESIS AND GENERATION OF CATIONIC POLYMER-TEMPLATED GOLD NANOPARTICLES BY IONIZING RADIATION

3.1 Introduction

Polymers have recently been investigated for functionalizing the surface of gold nanoparticles for different applications. Gold nanoparticles with polymer functionalized surfaces show increased stability, have controllable surface properties, and can be further surface modified to meet different requirements (Ramos & Rege, 2011). These properties make them attractive for therapeutic purposes.

In this work, five cationic polymers (generated in house) and pEI were investigated for their ability to form gold nanoparticles via radiolysis of water. The polymers were combined with metallic gold and nanopure water.

3.2 Materials and Methods

3.2.1 Materials. The amines 1,4-bis(3-aminopropyl) piperazine (1,4Bis), 3,3'-Diamino-Nmethyldipropylamine (3,3') and Pentaethylenehexamine (PHA) and the diglycidyl ethers Neopentyl glycol diglycidyl ether (NPGDE) and 1,4-Cyclyhexanedimethanol diglycidyl ether (1,4C) were purchased from Sigma Aldrich. Gold(III) chloride trihydrate ($HAuCl_4 \cdot 3H_2O$) was purchased from Sigma-Aldrich. Branched polyethyleneimine (pEI) (MW ~ 25,000Da) was also obtained from Sigma-Aldrich. All products were used as received.

3.2.2 Polymer Synthesis. Polymer synthesis was carried out as follows: briefly, 1,4C was reacted with PHA to form 1,4C-PHA, 1,4C was reacted with 1,4Bis to form 1,4C-1,4Bis, 1,4C was reacted with 3,3' to form 1,4C-3,3', NPGDE was reacted with PHA to form NPGDE-PHA, and NPGDE was reacted with 1,4Bis to form NPGDE-1,4Bis. The amines and diglycidyl ethers were reacted in equimolar amounts at room temperature in order to generate the cationic polymers listed above. The reaction mechanism is shown in **Figure 7**. The polymerization reaction was carried out in 20 mL glass scintillation vials for 16 hours. Polymers were dissolved at a concentration of 10 mg/mL in phosphate-buffered saline (0.01 X PBS) following the reaction. The solution pH was adjusted to 7.4 using 30% hydrochloric acid in de-ionized (DI) water. This was done in order to compensate for the basicity of the cationic polymer. Extent of polymerization was determined by comparing reactive amine concentrations at the initial mixing of monomer reagents and after 16 hours of polymerization. This was determined using the ninhydrin assay (Barua et. al, 2009).

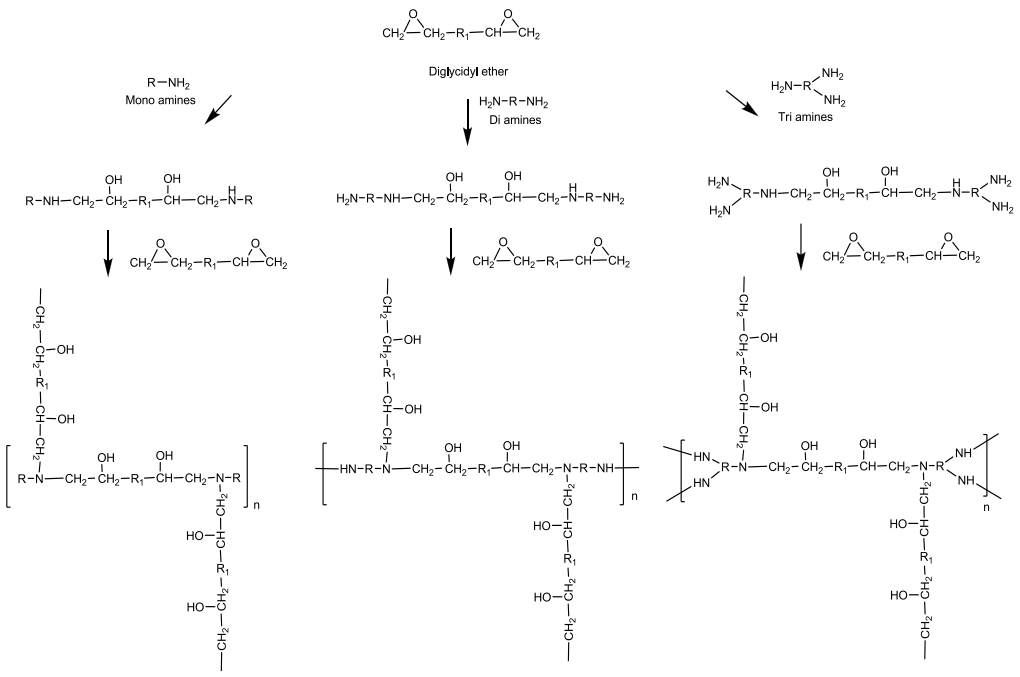

Figure 7: Reaction mechanism for formation of cationic polymers from amines and diglycidyl ethers.

3.2.3 Preparation of Samples for Irradiation. Samples were prepared as follows: $HAuCl_4$ ($1x10^{-3}$M) was mixed with cationic polymer (0.1% w/v) and the balance nanopure water (18.2 MΩ-cm, resistivity). Samples were mixed immediately prior to irradiation.

3.2.4 Sample Irradiation. Samples were transported to the Banner MD Anderson Cancer Center for irradiation tests. A Truebeam linear accelerator irradiated the samples to different doses, at a dose rate of ~15Gy/minute. The doses were 268Gy, 536Gy, 804Gy, and 1072Gy. After irradiation, samples were transported back to the lab for characterization.

3.2.5 Absorbance Spectroscopy. After irradiation, the absorbance spectra of the samples were measured. The absorbance was measured using a BioTek plate reader and Gen5 software. Absorbance measurements were read from 300nm to 995nm, with a step size of 5nm in a 96 well plate, with 150uL of sample in each well. The absorbance was measured at ~18 hours post irradiation.

3.3 Results and Discussion

3.3.1 Control Experiments. As mentioned in Chapter 2, the reactive species formed upon the radiolysis of water reduce the metallic gold to its zero valence state. In the absence of radiation, however, no gold nanoparticles are formed, as seen in the figures in **Appendix A**. This is not the case, though, for the cationic polymers. The amine groups present in the polymers are able to reduce the metallic gold to the zero valence state without needing radiation, as seen in **Figure 8**. The absorbance spectra for the control polymer experiments can be seen in **Appendix B**.

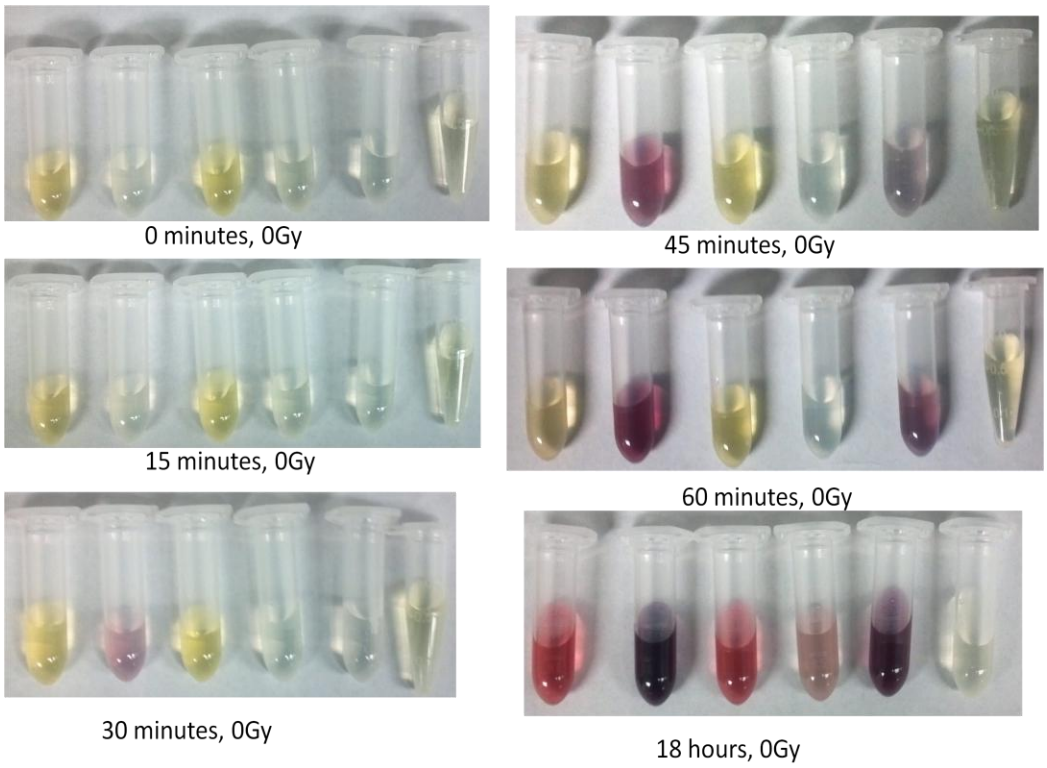

Figure 8: Cationic polymers, from left to right, 1,4C-PHA, NPGDE-1,4Bis, NPGDE-PHA, 1,4C-3,3', 1,4C-1,4Bis, and pEI. The polymer/gold salt solution had no gamma radiation added.

Of interest are the polymers that contain the amine 1,4Bis. Within 30 minutes of mixing, a color change is observed in NPGDE-1,4Bis, indicating that gold nanoparticle formation has started to occur, and within 45 minutes of mixing 1,4C-1,4Bis has started changing color. This was seen in each of the independent experiments performed with NPGDE-1,4Bis. While the phenomena is fascinating to observe, these polymer/ metallic gold mixtures would not be useful in a radiation sensing situation, as they change color without a radiation presence. The NPGDE-1,4Bis-Templated gold nanoparticles were not stable though for very long. The particles would fall out of solution, as observed on multiple

occasions after a couple of hours. Also of interest is the 1,4C-3,3' polymer. It shows no spontaneous color change in the first 60 minutes of mixing and only a slight color change after 18 hours of mixing. This polymer would perhaps be a good lead for more sensing experiments as it doesn't extensively form gold nanoparticles in the absence of radiation.

3.3.2 Effects of Radiation Dose. The experimental systems underwent a similar radiation dose treatment as the samples seen in Chapter 2, though not quite as extensive. The doses were kept to 268Gy, 536Gy, 804Gy, and 1072Gy. The effect of dose is seen in **Figure 9**.

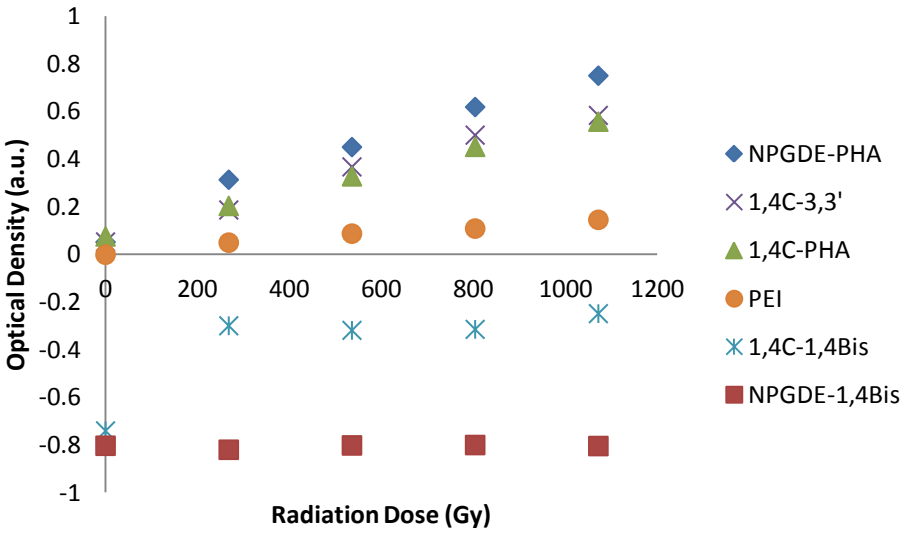

Figure 9: The effect of radiation dose on each of the polymers studied. Measurements were collected at 525nm. The spectra are corrected to not include the absorbance of the "no radiation" controls.

As is observed through **Figure 9**, the dose of radiation has an effect on the gold nanoparticle formation. As the dose increases, so does the optical density, indicating higher gold nanoparticle formation. Observe the NPGDE-1,4Bis

polymer: it has almost no optical density recorded. This is due to the unstable nanoparticles falling out of solution by the time the absorbance spectra were read. When the experimental samples are exposed to more radiation, they have more of the reactive species H·, ·OH, and e_{aq}- present in the system. Along with the amines present, due to the polymer, more metallic gold is reduced, giving rise to more gold nanoparticles formed.

3.4 Conclusion. In this chapter, gold nanoparticles Templated with cationic polymers were discussed. They were formed via the same method, radiolysis of water, as the gold nanoparticles discussed in Chapter 2. Unique to this chapter, though, was the ability of the cationic polymers to form gold nanoparticles in the absence of radiation. This was due to the amines present in the polymers. The amines were able to reduce the metallic gold to the zero valence state without needing the reactive species produced by the radiolysis of water. Some of the polymers, in particular those with the amine 1,4Bis, were able to reduce the metallic gold very quickly in the absence of radiation. These are not good candidates for sensing applications. However, the polymer 1,4C-3,3' presented itself as a promising lead for radiation sensing as it showed little color change in the absence of radiation.

Chapter 4

FUTURE WORK

4.1 Chapter 2 Future Work. For the work presented in Chapter 2, all of the radiation experiments have been completed. The work that should be performed next is extensive characterization of the samples. More absorbance spectra analysis should be conducted, possibly looking at the area under the curve and determining a physical representation of that analysis. Scanning electron microscopy (SEM) or Transmission electron microscopy (TEM) should be performed on the samples to give visual representation of the gold nanoparticles formed. As the work here shows, the lowest dose of radiation that the C_nELP/gold system can detect is 175Gy. This radiation dose is still quite high from a biological standpoint. A system that can detect low amounts of radiation needs to be determined. Modification to the ELP concentration should be studied along with working on modifying the ELP itself. Different thiol-containing compounds should also be considered for improving system sensitivity.

4.2 Chapter 3 Future Work. Future work to be conducted regarding the cationic polymer-Templated gold nanoparticle formation would include particle size determination, surface charge determination, and scanning/transmission electron microscopy (SEM/TEM) for characterization of the particles.

Lower-dose radiation experiments should be conducted to determine the lowest dose the present system can detect. If possible, the system should be optimized to detect radiation doses applicable in clinical settings.

Decreasing the polymer concentration should be studied, since at the present concentration, gold nanoparticles form in the absence of radiation. A polymer screen should also be conducted to determine other lead polymers that could be used to detect ionizing radiations, like gamma rays and X-rays.

REFERENCES

Barua, S., Joshi, A., Banerjee, A., Matthews, D., Sharfstein, S. T., Cramer, S. M., et al. Parallel Synthesis and Screening of Polymers for Nonviral Gene Delivery. *Molecular Pharmaceutics,2009 6*(1), 86-97.

Huang, H.-C.; Koria, P.; Parker, S. M.; Selby, L.; Megeed, Z.; Rege, K. Optically Responsive Gold Nanorod,aì Ṕ olypeptide Assemblies. *Langmuir, 2008 24* (24), 14139−14144.

Huang, H.-C.; Yang, Y.; Nanda, A.; Koria, P.; Rege, K. Synergistic administration of photothermal therapy and chemotherapy to cancer cells using polypeptide-based degradable plasmonic matrices. *Nanomedicine, 2011 6* (3), 459−473.

Lahtz, C., Bates, S. E., Jiang, Y., Li, A. X., Wu, X., Hahn, M. A., & Pfeifer, G. P. Gamma irradiation does not induce detectable changes in dna methylation directly following exposure of human cells. *PLOS One, 2012 7*(9), 1-8.

Liu, Z., Xue, Wangxin, et. al. A facile and convenient fluorescence detection of gamma-ray radiation based on the aggregation-induced emission. *Journal of Materials Chemistry, 2011 21*, 14487-14491.

Meyer, D. E.; Chilkoti, A. Genetically encoded synthesis of protein-based polymers with precisely specified molecular weight and sequence by recursive directional ligation: examples from the elastinlike polypeptide system. *Biomacromolecules, 2002 3*(2), 357−67.

Misra, N., Biswal, J., Gamma radiation induced synthesis of gold nanoparticles in aqueous polyvinyl pyrrolidone solution and its application for hydrogen peroxide estimation. *Radiation Physics and Chemistry, 2012 81*, 195-200.

Nath, N.; Chilkoti, A. Interfacial phase transition of an environmentally responsive elastin biopolymer adsorbed on functionalized gold nanoparticles studied by colloidal surface plasmon
resonance. J. *Am. Chem. Soc., 2001 123* (34), 8197−8202.

Ramos, J., & Rege, K.. Transgene delivery using poly(amino ether)-gold nanorod assemblies.*Biotechnology and Bioengineering, 2011 109*(5), 1336-1346.

Urry, D. W. Physical Chemistry of Biological Free Energy Transduction As Demonstrated by Elastic Protein-Based Polymers. *J. Phys. Chem. B, 1997 101* (51), 11007−11028.

Washington, C. M., & Leaver, D. (2010). *Principles and practice of radiation therapy*. (3rd ed.). St. Louis: Mosby Elsevier.

APPENDIX A

C_NELP-TEMPLATED GOLD NANOPARTICLE CONTROL AND LOW DOSE RADIATION DATA

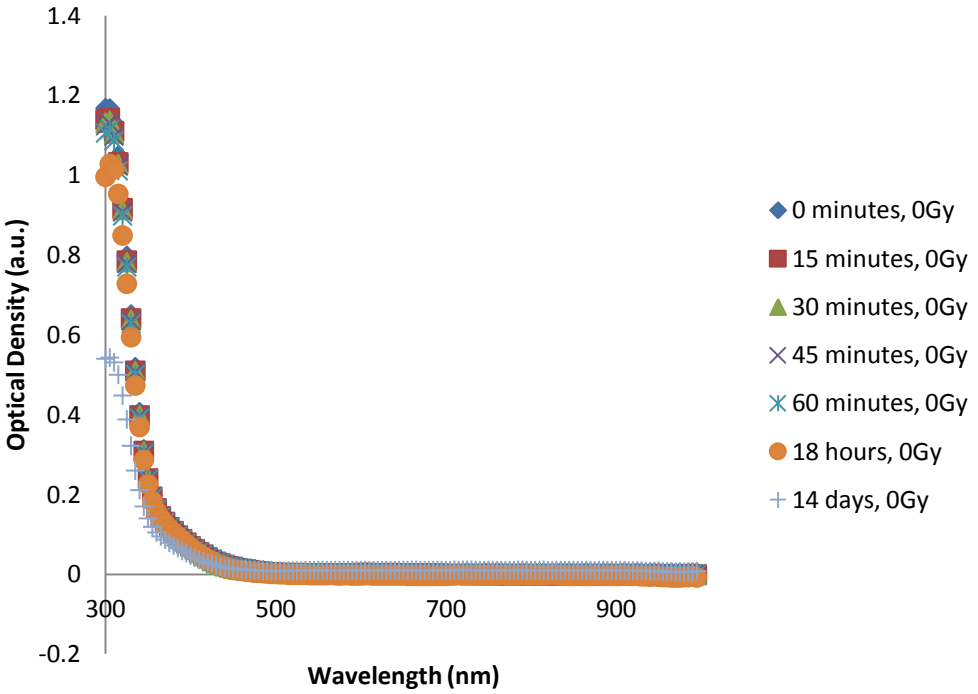

Figure A1: C_2ELP with metallic gold, IPA, acetone, and nanopure water with no radiation.

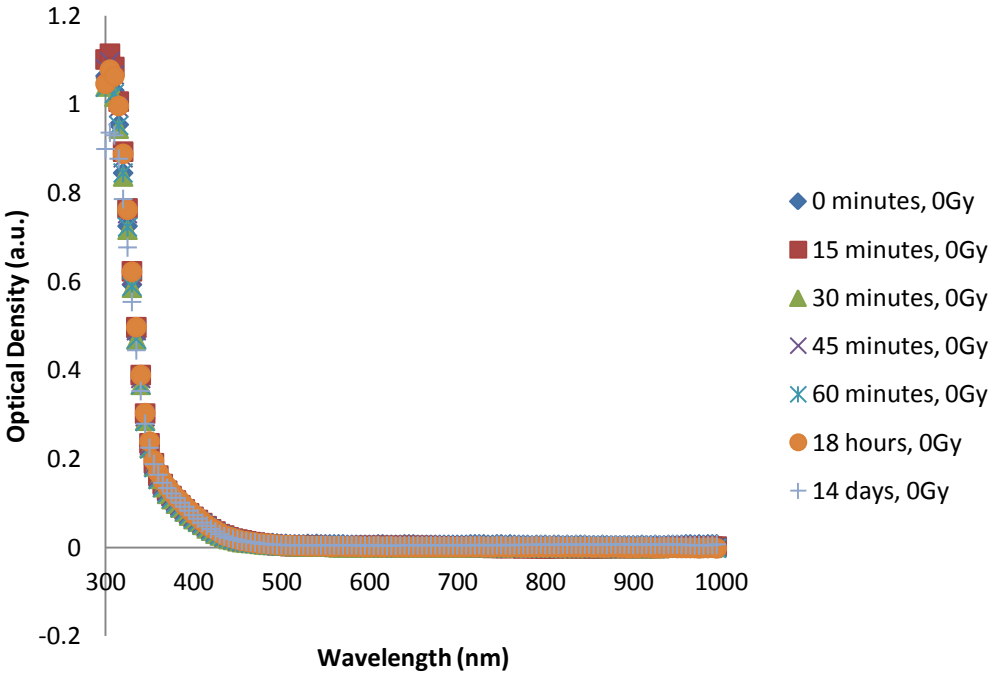

Figure A2: C_2ELP with metallic gold and nanopure water with no radiation.

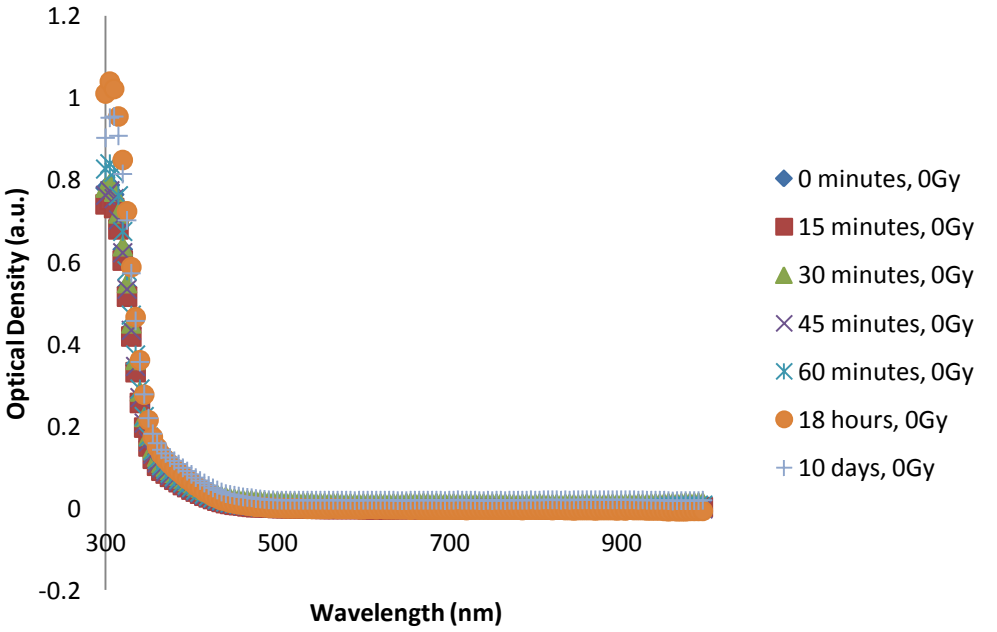

Figure A3: C_{12}ELP with metallic gold, IPA, acetone, and nanopure water with no radiation.

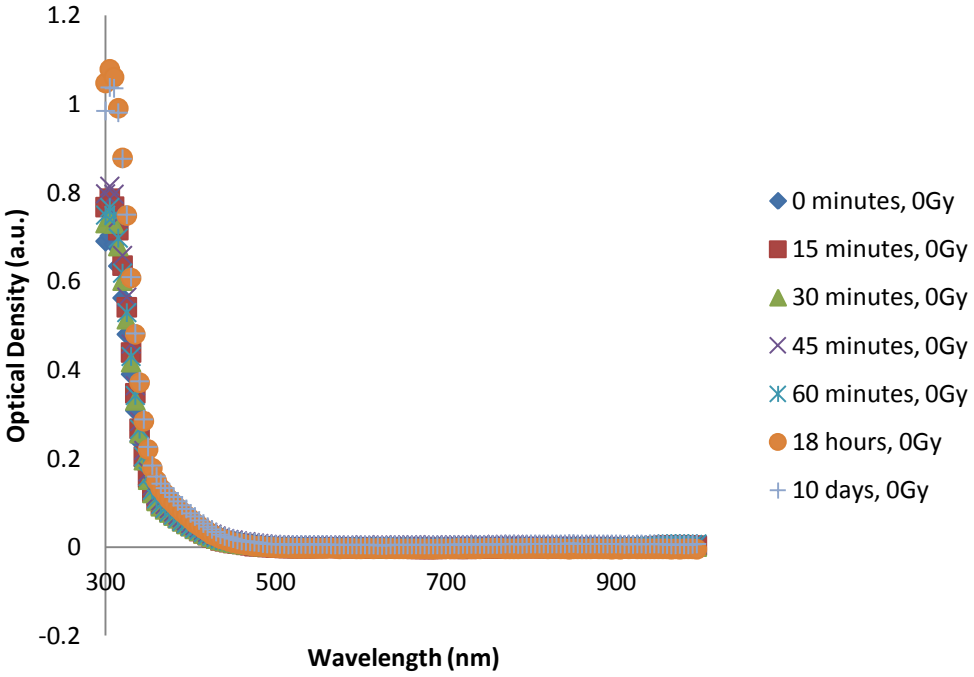

Figure A4: C_{12}ELP with metallic gold and nanopure water with no radiation.

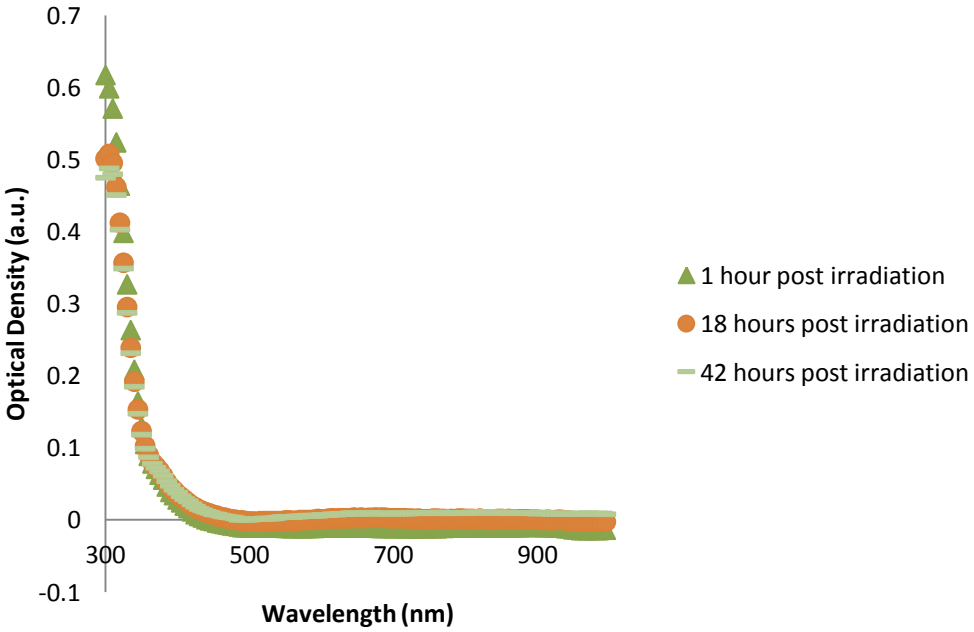

Figure A5: C_2ELP with 0.5Gy radiation dose.

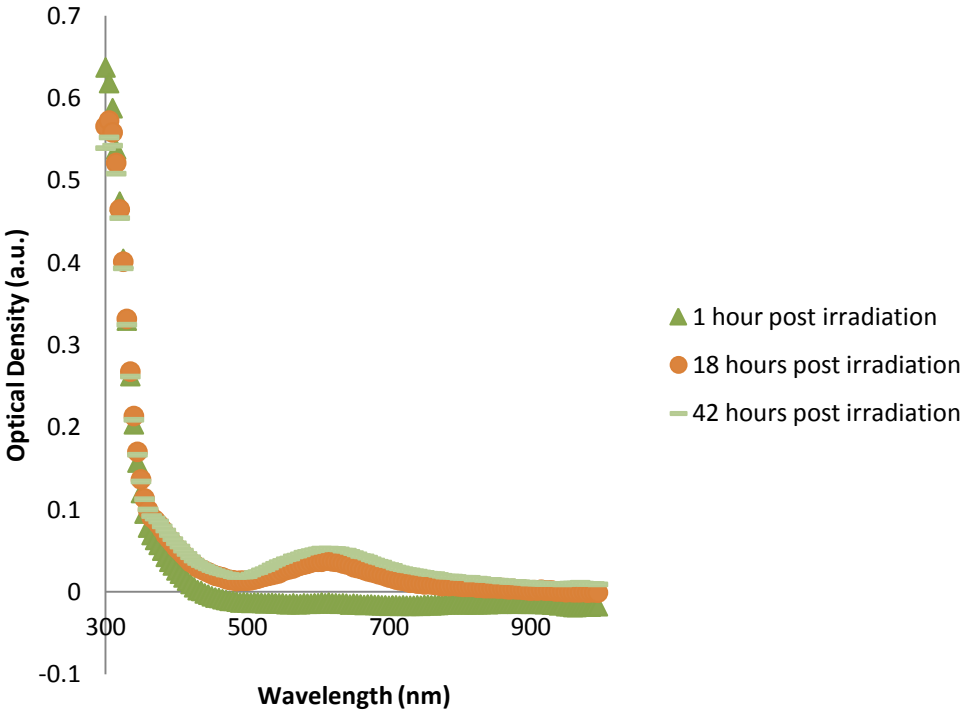

Figure A6: C_2ELP with 2Gy radiation dose.

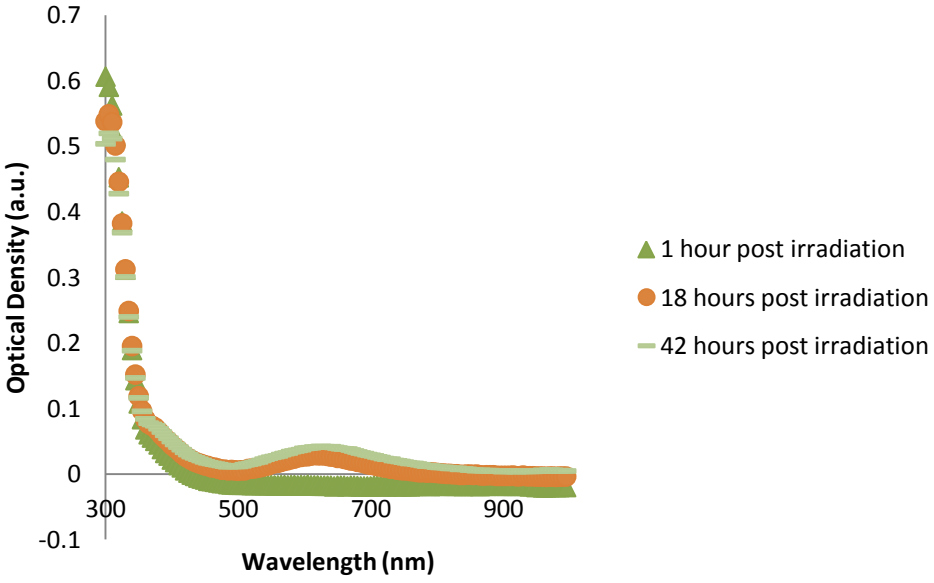

Figure A7: C_2ELP with 5Gy radiation dose.

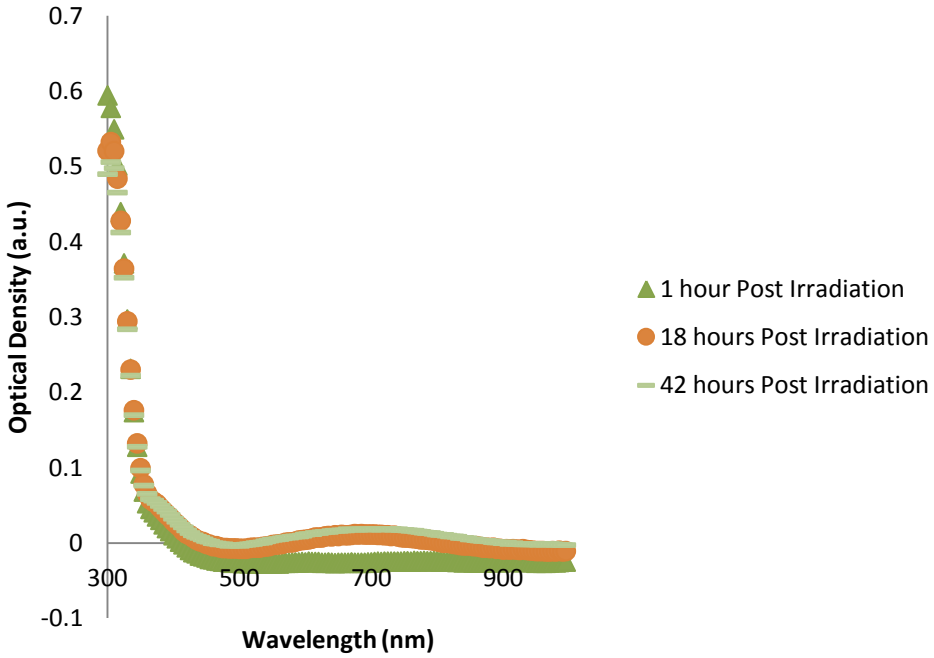

Figure A8: C_2ELP with 10Gy radiation dose.

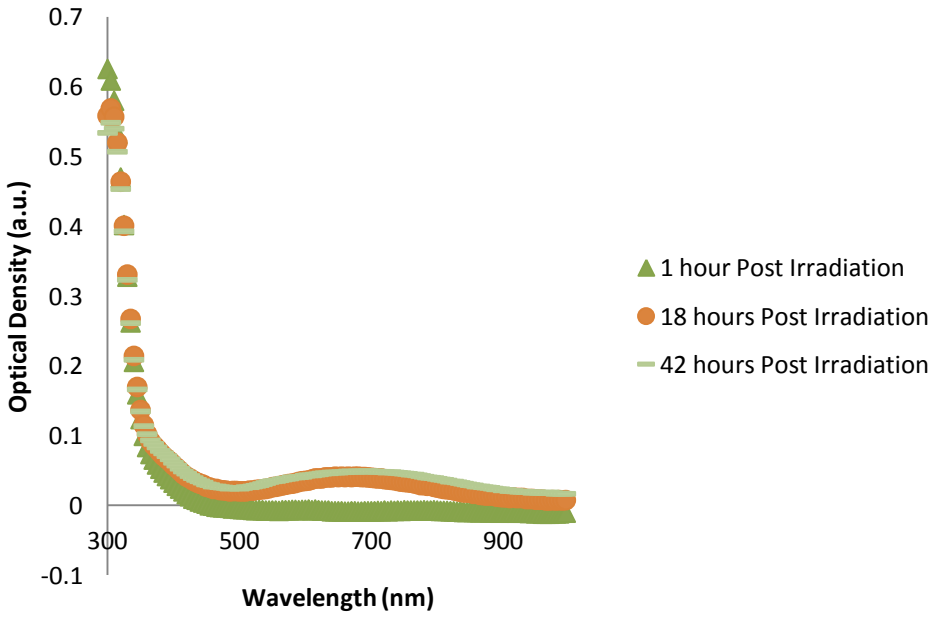

Figure A9: C_2ELP with 25Gy radiation dose

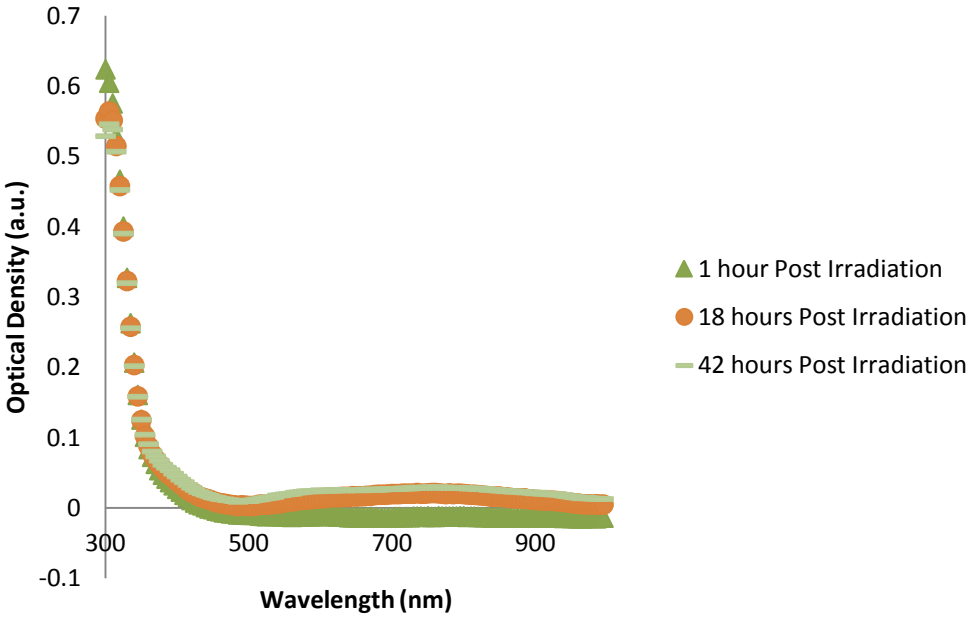

Figure A10: C_2ELP with 50Gy radiation dose

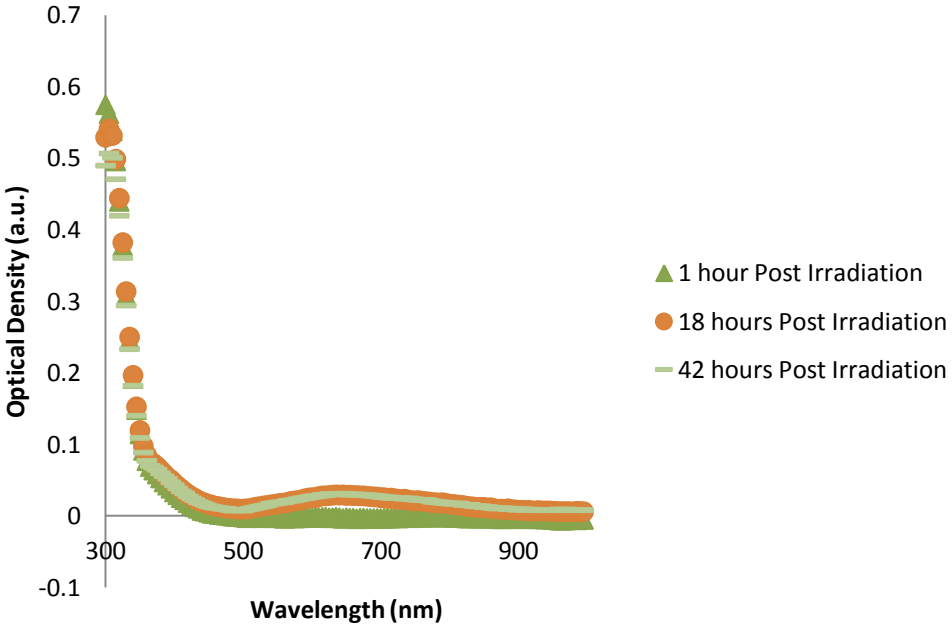

Figure A11: C_2ELP with 100Gy radiation dose

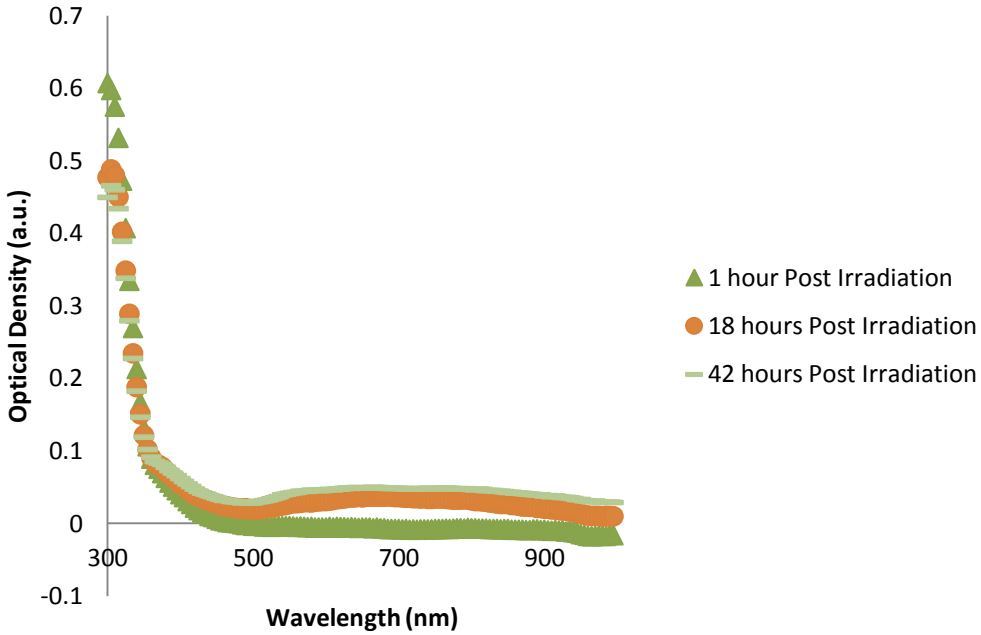

Figure A12: C_{12}ELP with 0.5Gy radiation dose

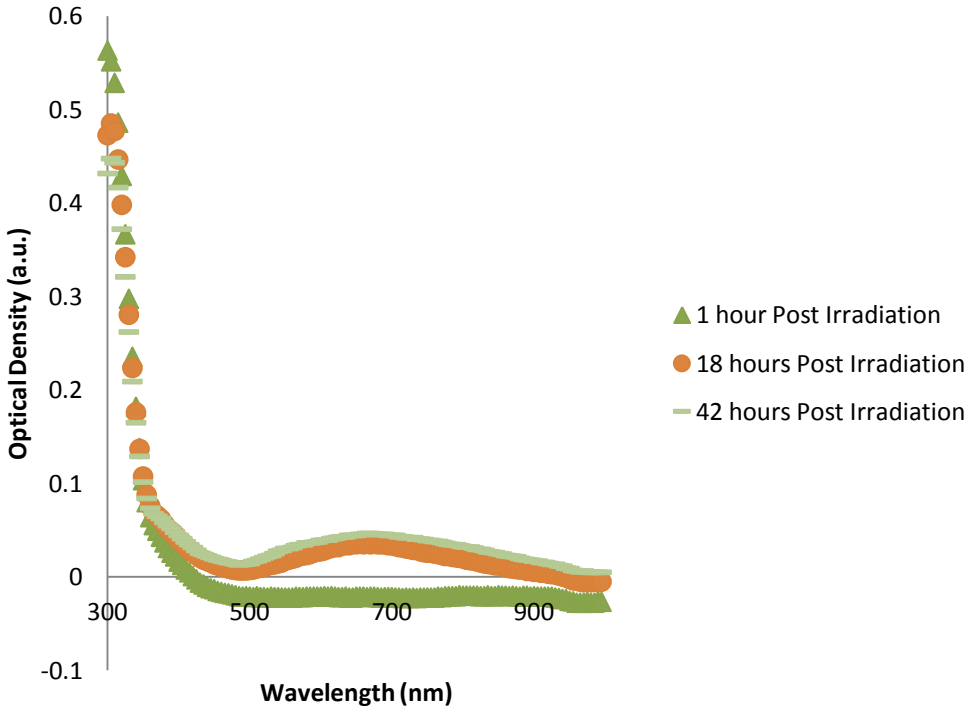

Figure A13: C_{12}ELP with 2Gy radiation dose

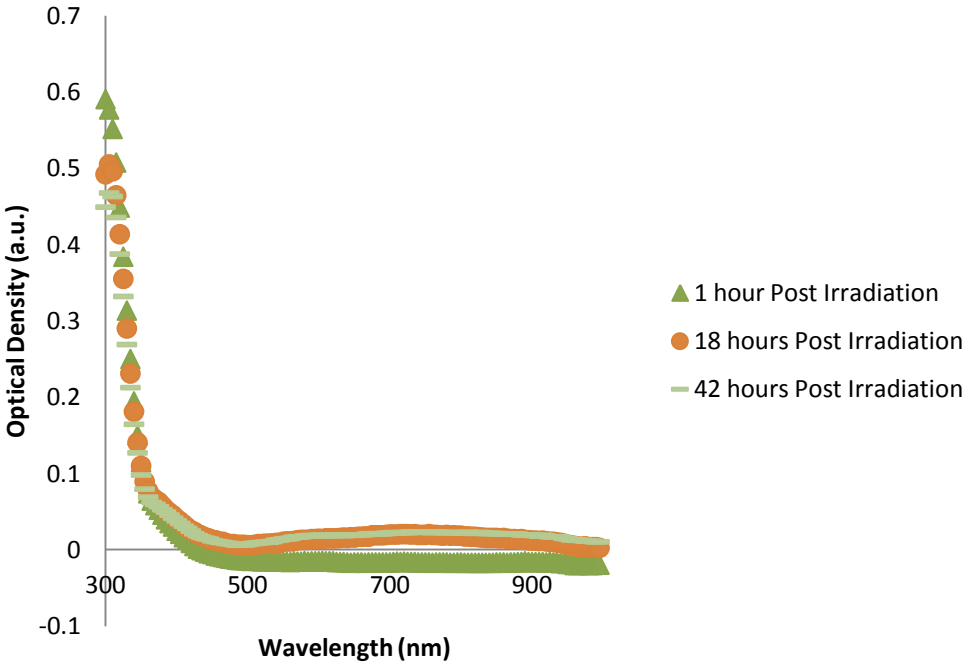

Figure A14: C_{12}ELP with 5Gy radiation dose

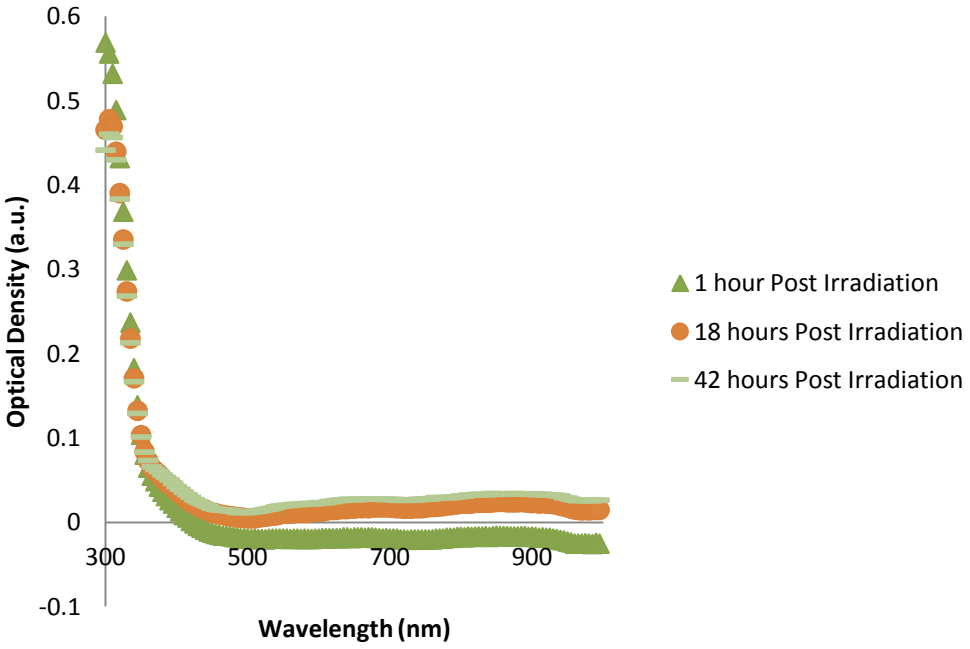

Figure A15: C_{12}ELP with 10Gy radiation dose

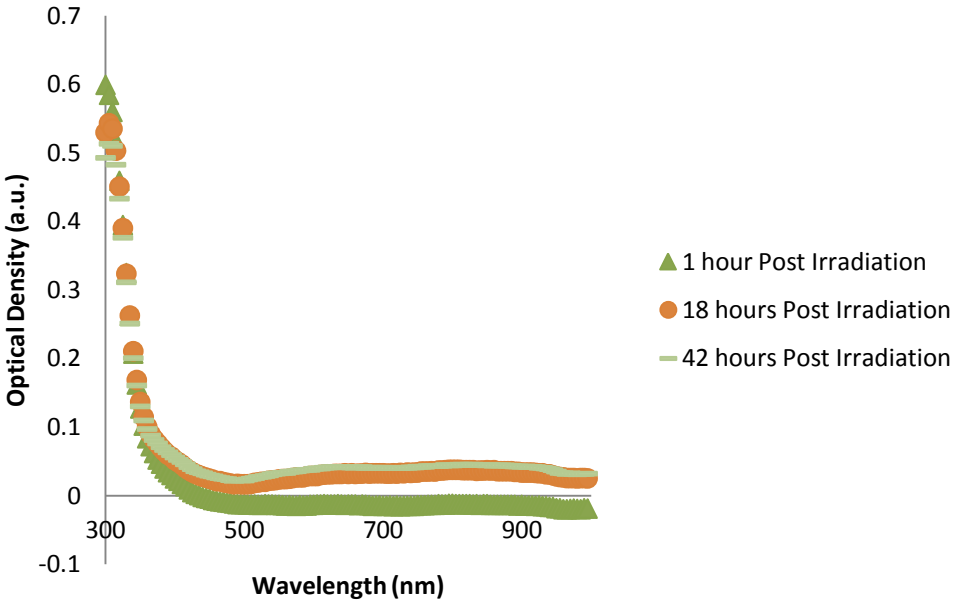

Figure A16: C_{12}ELP with 25Gy radiation dose

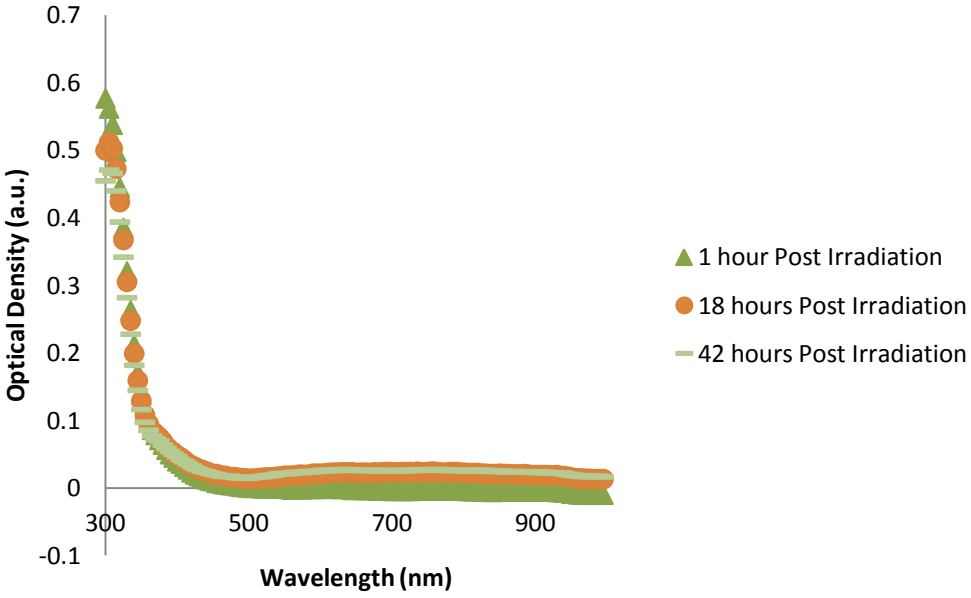

Figure A17: C_{12}ELP with 50Gy radiation dose

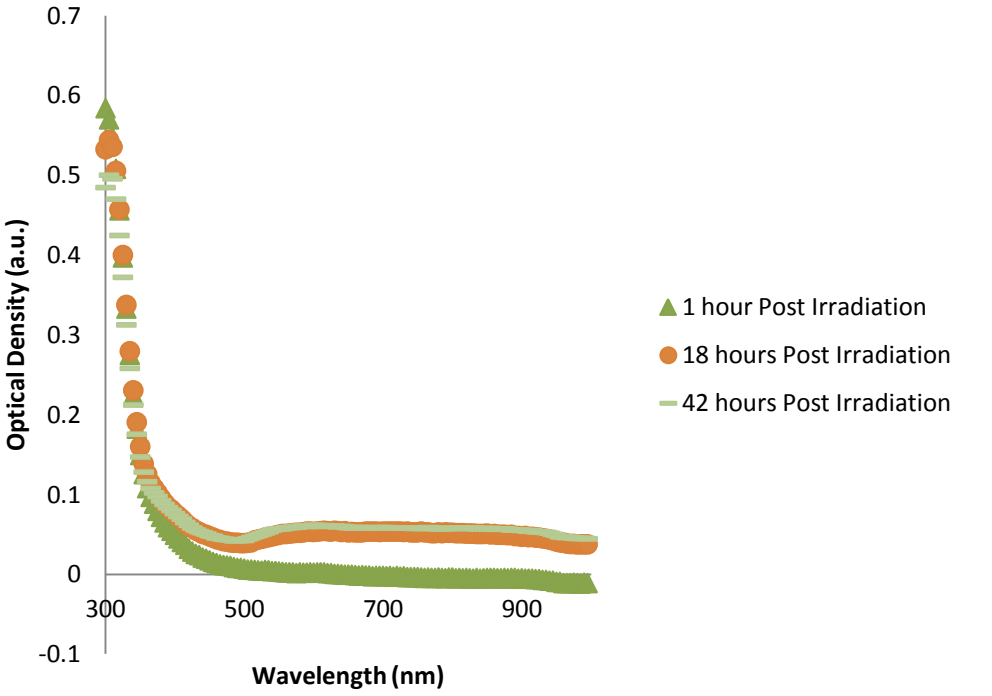

Figure A18: C_{12}ELP with 100Gy radiation dose

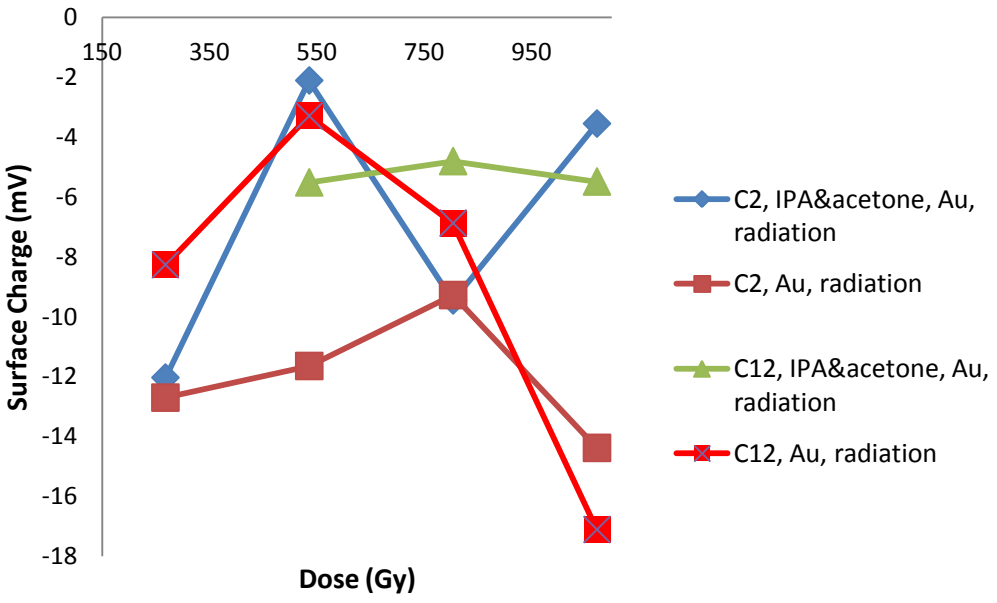

Figure A19: Preliminary zeta potential measurements showing particle surface charge is between -2mV and -17mV.

APPENDIX B

CATIONIC POLYMER-TEMPLATED GOLD NANOPARTICLE CONTROL AND EXPERIMENTAL DATA

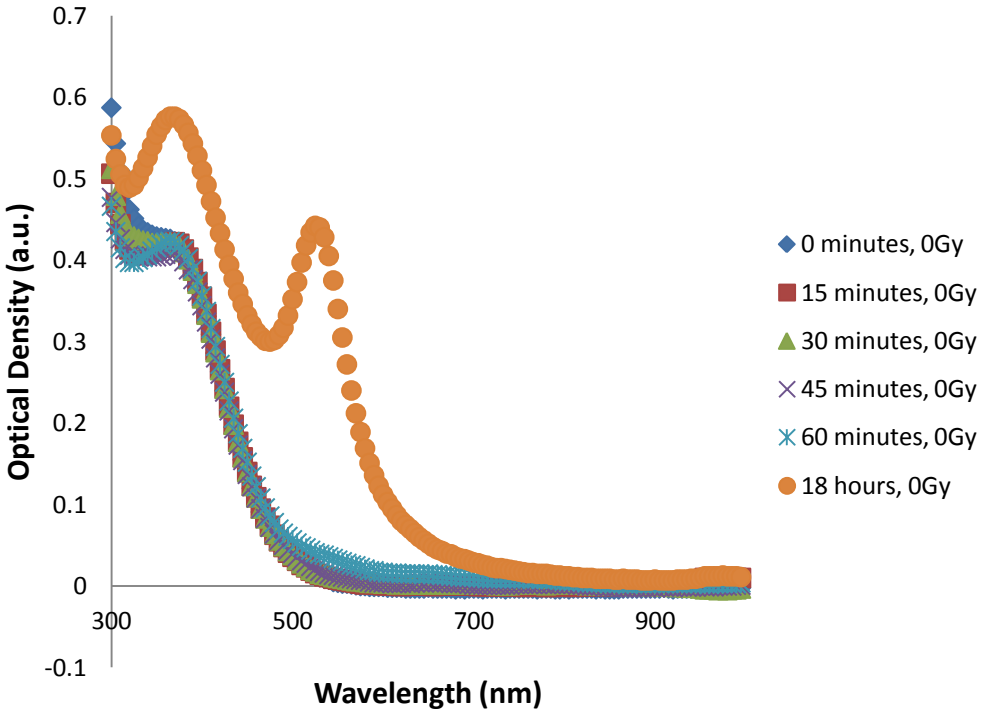

Figure B1: Absorbance spectra of 1,4C-PHA over an hour with no exposure to gamma radiation.

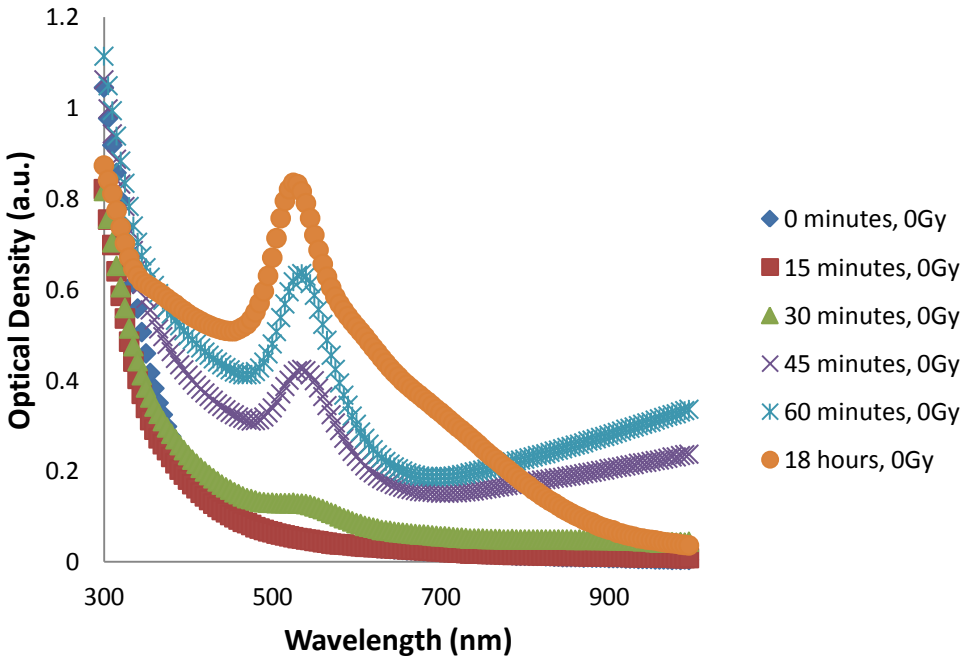

Figure B2: Absorbance spectra of NPGDE-1,4Bis over an hour with no exposure to gamma radiation.

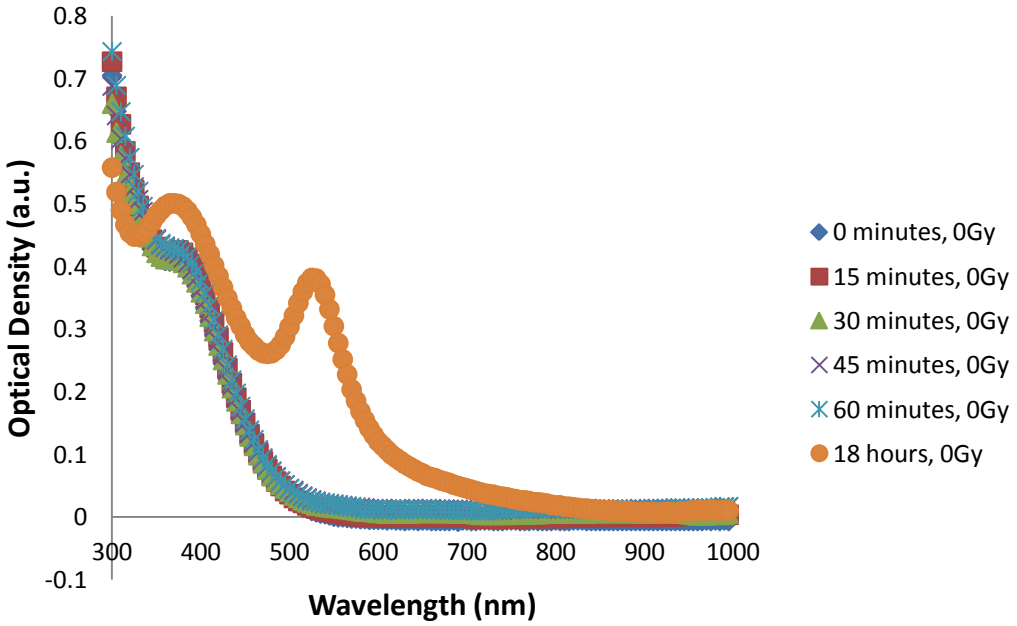

Figure B3: Absorbance spectra of NPGDE-PHA over an hour with no exposure to gamma radiation.

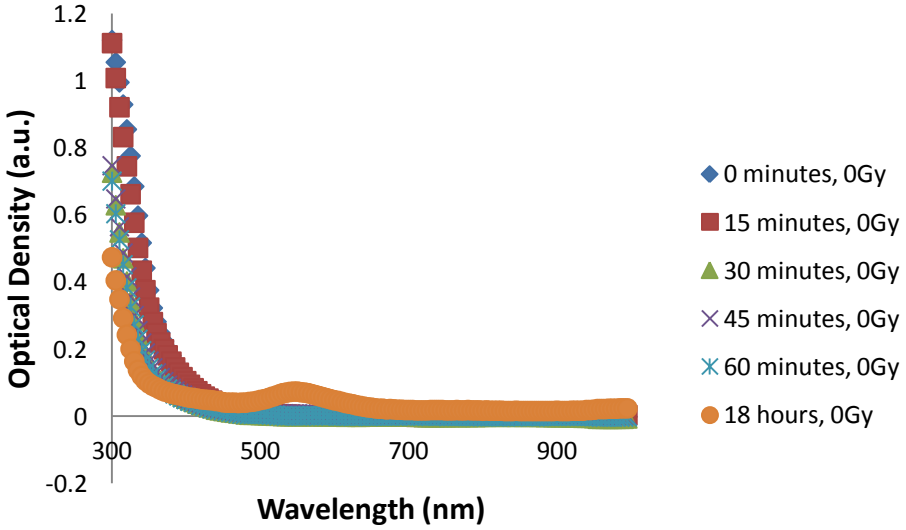

Figure B4: Absorbance spectra of1,4C-3,3' over an hour with no exposure to gamma radiation.

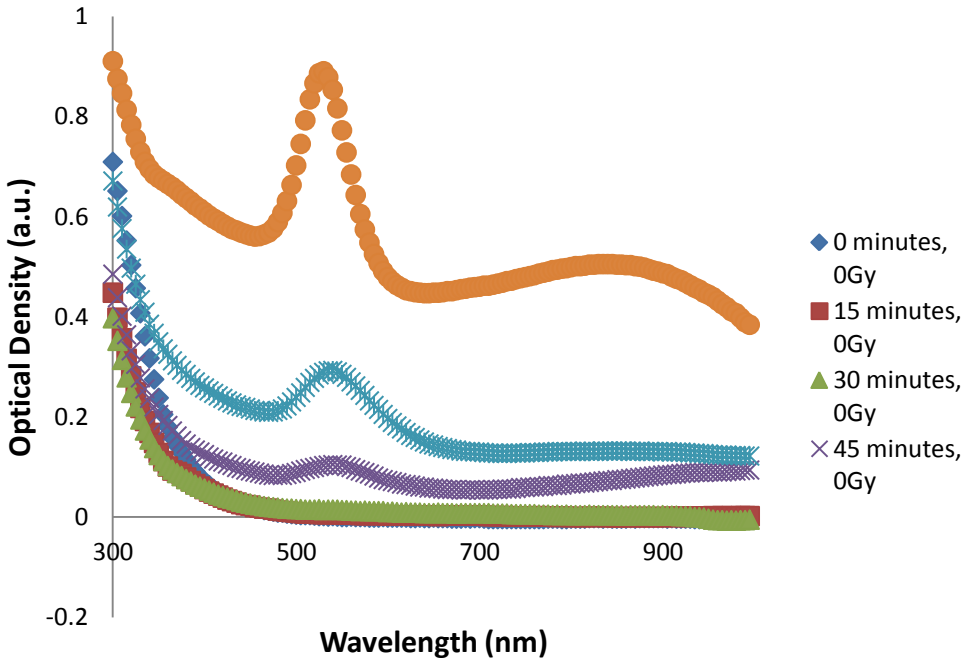

Figure B5: Absorbance spectra of1,4C-1,4Bis over an hour with no exposure to gamma radiation.

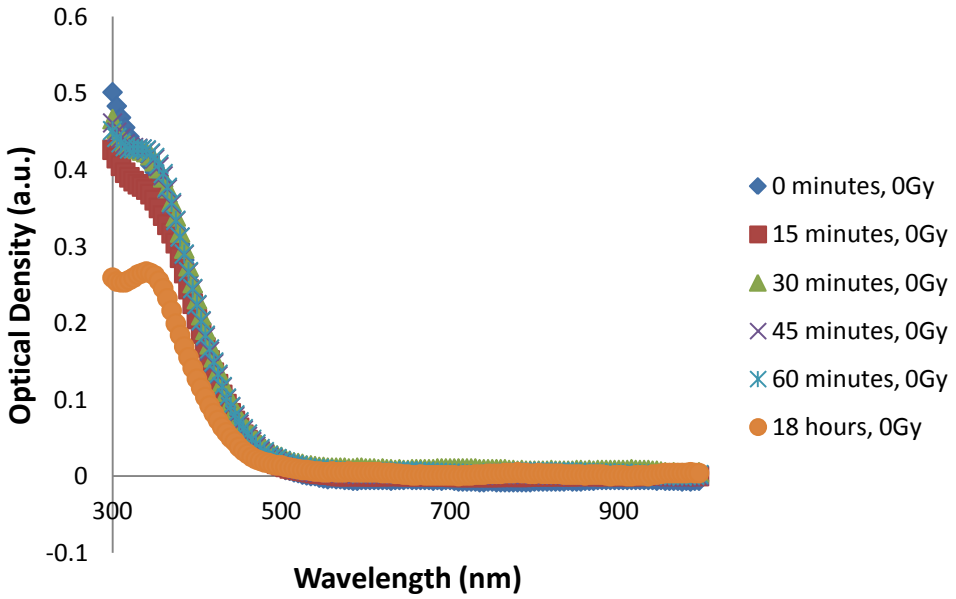

FigureB6: Absorbance spectra of pEI over an hour with no exposure to gamma radiation.

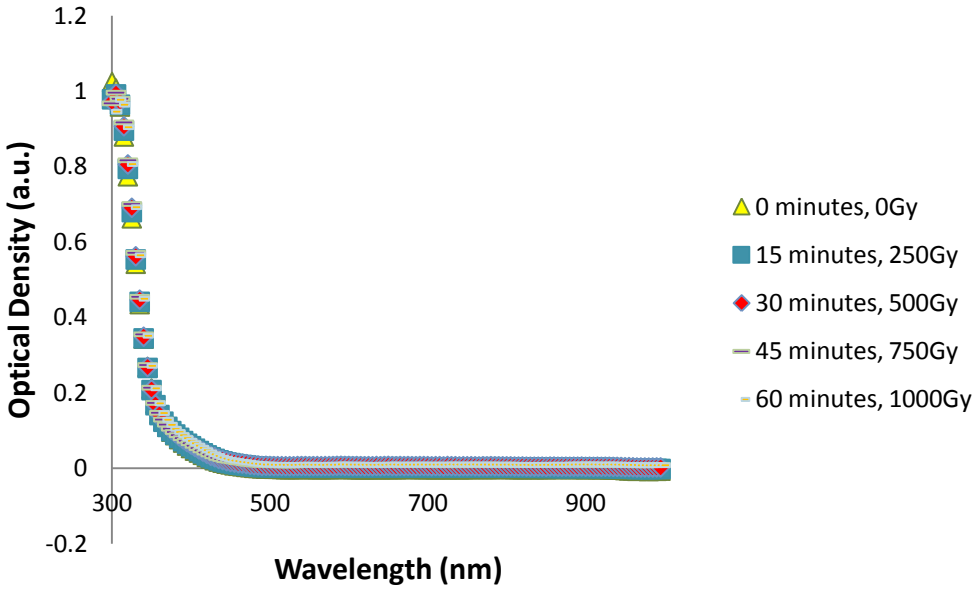

Figure B7: Metallic gold with nanopure water with radiation.

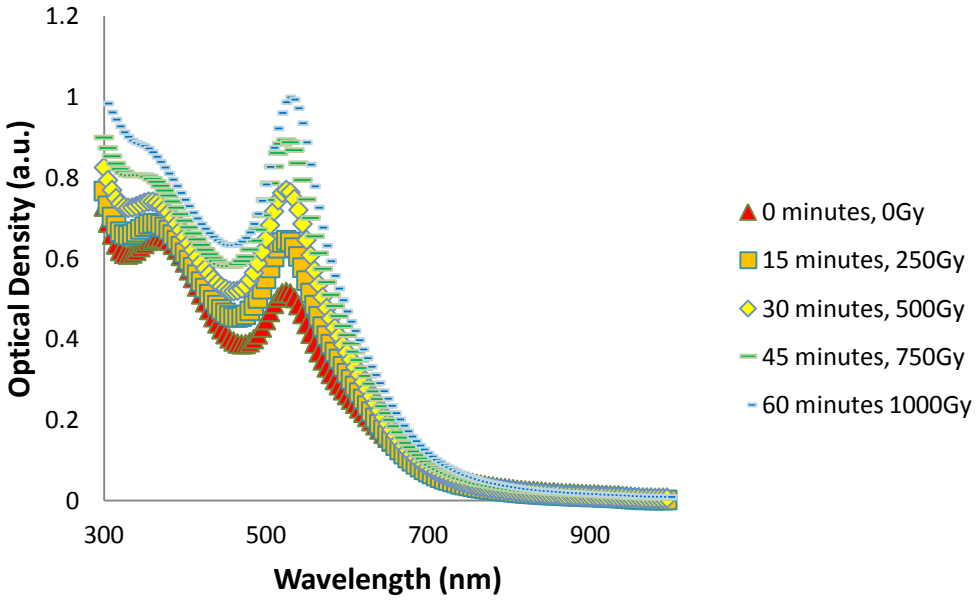

Figure B8: 1,4C-PHA with metallic gold and nanopure water with radiation.

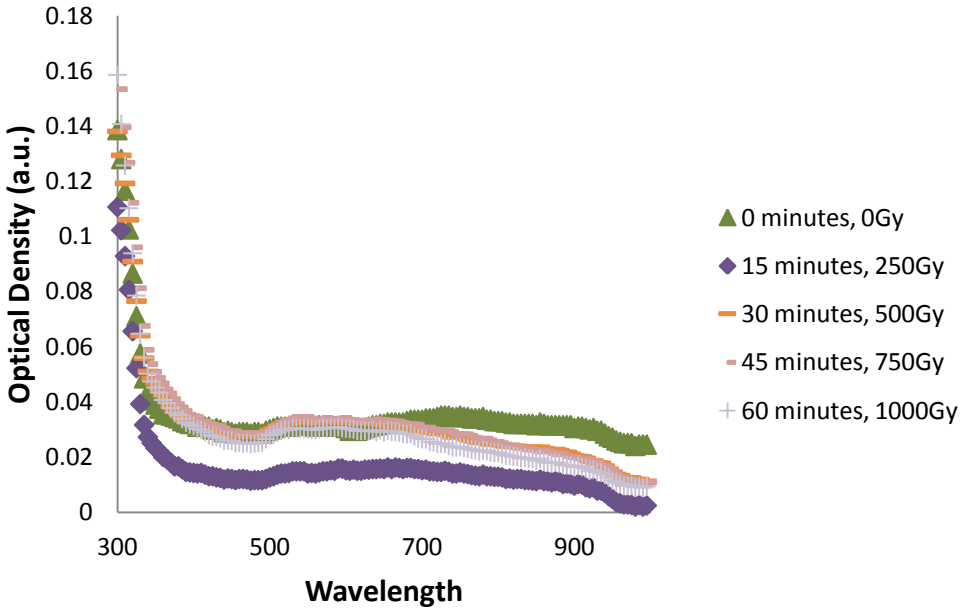

FigureB9: NPGDE-1,4Bis with metallic gold and nanopure water with radiation.

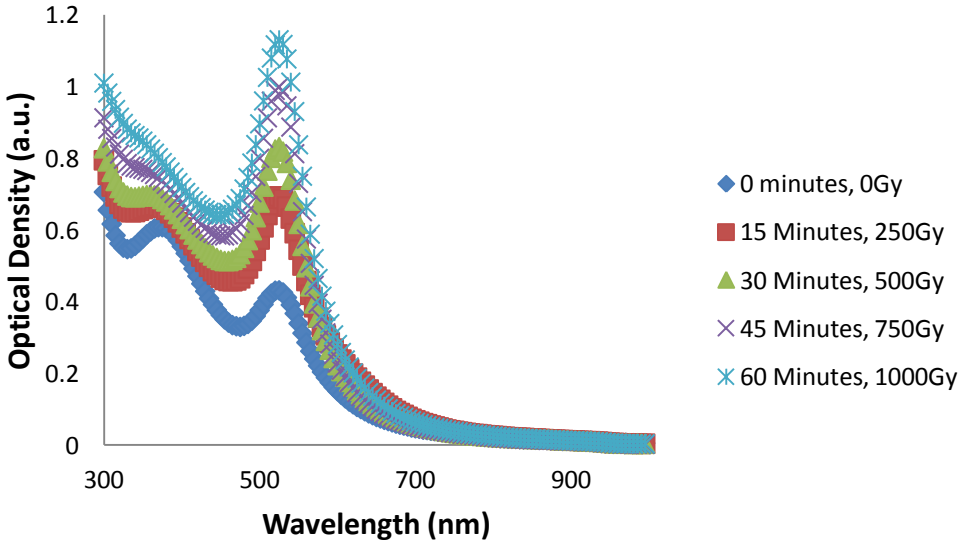

Figure B10: NPGDE-PHA with metallic gold and nanopure water with radiation.

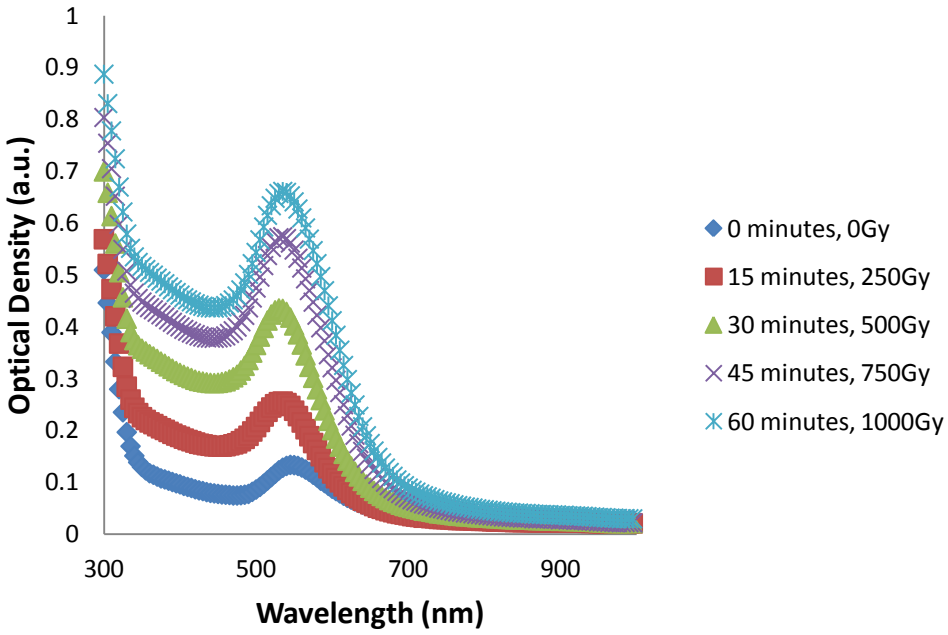

Figure B11: 1,4C-3,3' with metallic gold and nanopure water with radiation.

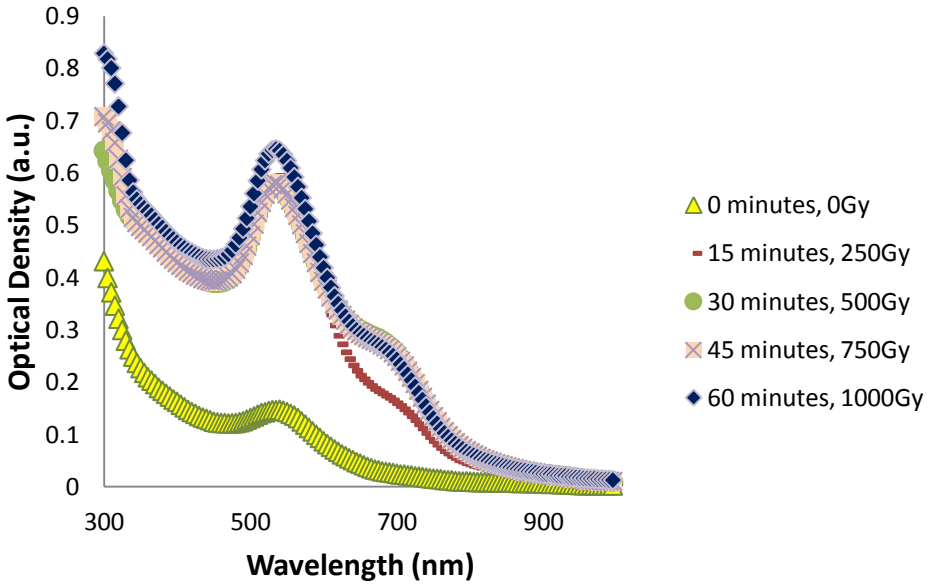

Figure B12: 1,4C-1,4Bis with metallic gold and nanopure water with radiation.

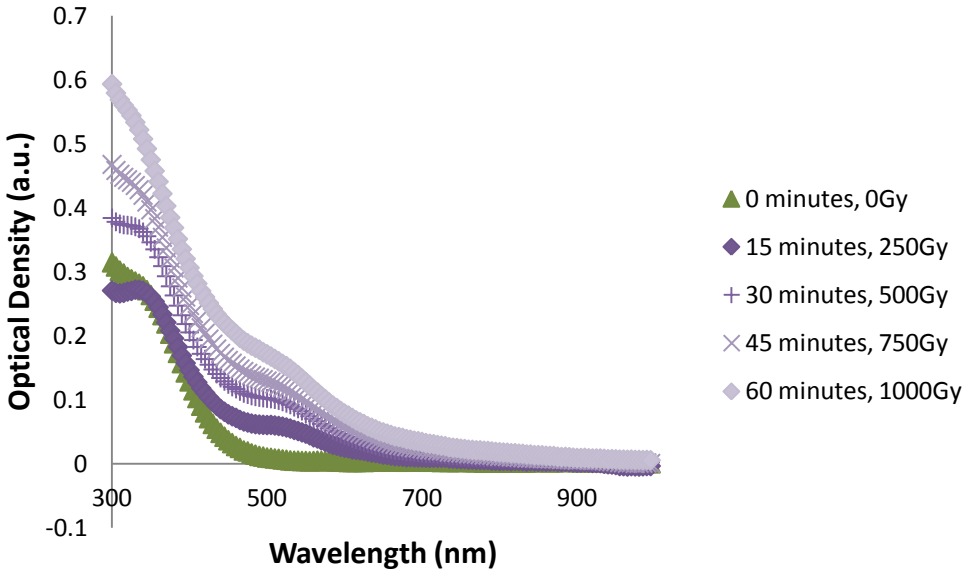

Figure B13: pEI with metallic gold and nanopure water with radiation.

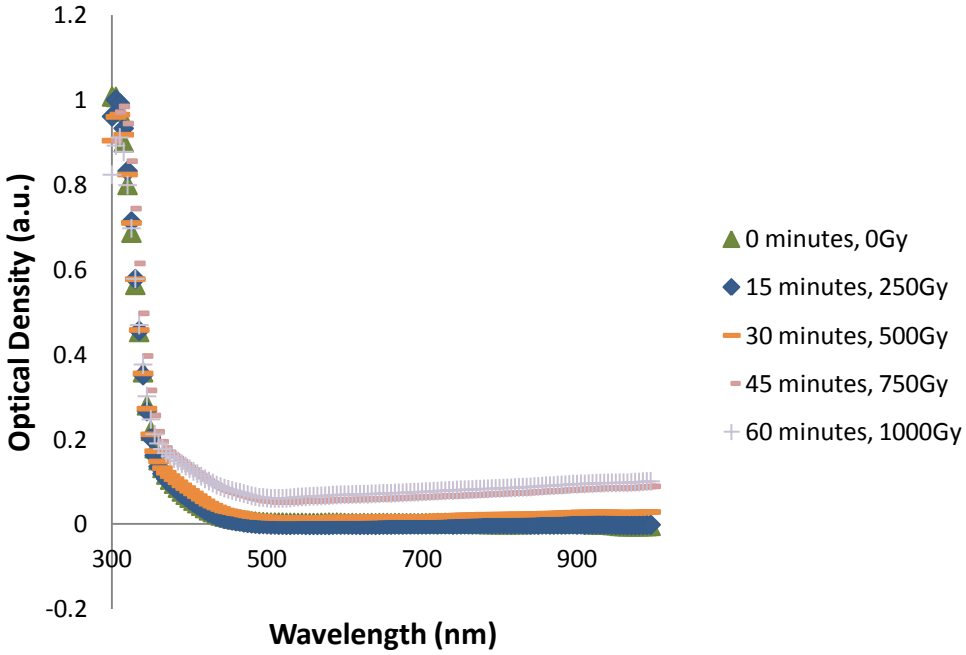

Figure B14: Metallic gold with IPA, acetone, and nanopure water with radiation.